WORKING PAPER · NO. 2020-72

Epidemic Responses Under Uncertainty

Michael Barnett, Greg Buchak, and Constantine Yannelis

MAY 2020

Becker Friedman Institute
FOR ECONOMICS AT UCHICAGO

5757 S. University Ave.
Chicago, IL 60637
Main: 773.702.5599
bfi.uchicago.edu

Epidemic Responses Under Uncertainty*

Michael Barnett
Arizona State University
W.P. Carey School of Business

Greg Buchak
Stanford University
Graduate School of Business

Constantine Yannelis
University of Chicago
Booth School of Business

May 2020

Abstract

We examine how policymakers should react to a pandemic when there is significant uncertainty regarding key parameters relating to the disease. In particular, this paper explores how optimal mitigation policies change when incorporating uncertainty regarding the Case Fatality Rate (CFR) and the Basic Reproduction Rate ($\mathcal{R}_0$) into a macroeconomic SIR model in a robust control framework. This paper finds that optimal policy under parameter uncertainty generates an asymmetric optimal mitigation response across different scenarios: when the disease's severity is initially underestimated the planner increases mitigation to nearly approximate the optimal response based on the true model, and when the disease's severity is initially overestimated the planner maintains lower mitigation as if there is no uncertainty in order to limit excess economic costs.

JEL: E1, H0, I1
Keywords: COVID-19, Coronavirus, Model Uncertainty, Dynamic General Equilibrium

*We are grateful to Scott Baker, Nick Bloom, Buz Brock and Lars Hansen for helpful comments and discussions. This draft is preliminary and incomplete, comments are welcome.

1 Introduction

The rapid spread of COVID-19 in 2020 was accompanied by a vigorous debate about the costs and benefits of severe actions taken to mitigate the spread of the pandemic. This debate was conducted with significant uncertainty about key parameters relating to the costs of the new virus, including death rates, infection rates and the economic costs of policies such as shuttering businesses and issuing shelter-in-place orders (Chater, 2020)[1]. Many policymakers and commentators in the media used the fact that there was significant uncertainty about the effects of COVID-19 to argue that this should lead to a more lax policy response, keeping businesses open and allowing free movement.[2] It is far from obvious, however, how uncertainty regarding the fundamentals of a potential threat should alter the optimal policy response. This paper explores how the economic and public health consequences of pandemic mitigation policies should be assessed in the face of significant uncertainty.

Determining the optimal response to COVID-19 is a prime example of policy makers having to make decisions with significant amounts of uncertainty. Even several months into the pandemic, there remained significant disagreement regarding key parameters relating to the damages of the new virus. In Epidemiology, two factors are particularly important for evaluating the severity of a contagious disease: first, the Case Fatality Rate (CFR), or the fraction of individuals infected who die due to the disease; second, the basic reproduction number $\mathcal{R}_0$, or the number of people in an otherwise healthy population that a single disease carrier is expected to infect. For example, estimates of the CFR ranged from being close to that of the seasonal flu, to two orders of magnitude higher than a seasonal flu. Estimates of $\mathcal{R}_0$ varied widely due to difficulty in measuring how many people were infected, in part due to the presence of a large number of asymptomatic carriers.[3] This uncertainty made it difficult for policy makers to weigh the health benefits of policies such as lockdowns against

[1] Early estimates of the Case-Fatality Rate (CFR) ranged from .08% to 13.04%. Estimates of the number of individuals each carrier infects, $\mathcal{R}_0$, ranged from 1.5 to 12 (Korolev, 2020)

[2] For example, the Mayor of New York Bill De Blasio noted in a March 9 press conference when asked whether the city would cancel a St. Patrick's day parade that "*I am very resistant to take actions that we're not certain would be helpful, but that would cause people to lose their livelihoods.*"

[3] The wide range of estimates is discussed in Manski and Molinari (2020) who derive bounds for parameters: "*In the present absence of random testing, various researchers have put forward point estimates and forecasts for infection rates and rates of severe illness derived in various ways... The assumptions vary substantially and so do the reported findings... We find that the infection rate as of April 6, 2020, for Illinois, New York, and Italy are, respectively, bounded in the intervals [0.001, 0.517], [0.008, 0.645], and [0.003, 0.510].*"

their economic damages.

The uncertainty about the effects of the virus on health outcomes has led some policymakers to suggest taking less severe steps to stem the spread of the virus. This sentiment was expressed by the well-known epidemiologist John Ioannides who noted in a widely-read opinion piece saying that

> *"In the absence of data, prepare-for-the-worst reasoning leads to extreme measures of social distancing and lockdowns. Unfortunately, we do not know if these measures work.... This has been the perspective behind the different stance of the United Kingdom keeping schools open, at least until as I write this. In the absence of data on the real course of the epidemic, we don't know whether this perspective was brilliant or catastrophic."*

Despite this and similar commentary from some policymakers suggesting that significant uncertainty should prevent drastic measures from being taken, economic theory would in fact suggest that the opposite conclusion is true. Higher levels of uncertainty should lead policymakers to avoid large losses, adopting a "maxmin" criterion (Hansen and Sargent, 2001) by selecting the policy that would be optimal under the worst-case scenario. Of course, the selection of the worst-case scenario itself must be disciplined by what is reasonably consistent with the data: For example, an extremely contagious disease with an eventual 100% fatality rate is indeed a worst-case scenario, but—parameter uncertainty notwithstanding—is not consistent with even the most pessimistic estimates. A CFR of 10%, however, while towards the extreme end of estimates, may be a reasonable worst-case scenario to consider. In this paper, we examine the smooth ambiguity and robust control approaches, which provide analytical frameworks to select a reasonable worst-case scenario to inform optimal policy decisions.

We embed parameter uncertainty into a simple macroeconomic model featuring a pandemic. In the model, policy-makers must weigh the health benefits of quarantine against economic damages inflicted by these policies. We begin with a standard Susceptible, Infectious, or Recovered[4] (SIR) model augmented by Brownian motions. These Brownian shocks capture not only randomness in the spread of the disease, but importantly, difficulties in measuring infections and classifying deaths. These perturbations make it difficult

[4]SIR models are standard tools in epidemiology used to model the spread of infectious diseases. The epidemiological SIR model computes the theoretical number of people infected with a contagious disease in a closed population over time. The models have three key elements: S is the number of susceptible, I is the number of infectious, and R is the number of recovered, deceased, or immune individuals. A recent literature in macroeconomics incorporates SIR models into macroeconomics models. Stanford Earth System Sciences notes provide a introduction to the standard epidemiological SIR model.

for a policy maker to infer the true parameter values underlying the disease's spread and case severity, meaning that the policy maker must make policy decisions knowing that her model is ambiguously specified or potentially misspecified. We compare optimal policies as well as public health and economic outcomes in a model that explicitly takes this potential ambiguity or misspecification into account. We calibrate the model to match the US economy, and explore how uncertainty influences optimal quarantine policy.

We find that more uncertainty about parameters of a disease—death rates and reproduction rates—leads a policy maker to optimally adopt a harsher quarantine in most situations. This is particularly true when the policy maker's initial prior on the disease's severity is low and it is allowed to spread. As relatively large portions of the population become infected, the cost of underestimating the disease increases. This is because in a worst-case scenario, the pool of already-infected people will lead to significantly more infections and death than if the pool of potential spreaders was much smaller. Thus, when there is more uncertainty about the impact of a new virus, the government should do more to combat the spread. The intuition for this finding is that the planner seeks to avoid the worst possible outcomes, in case the uncertainty resolves in an adverse way.

There is an economically important asymmetry that we find when the policy maker's initial prior on the disease's severity is high. Because far smaller portions of the population become infected than the prior model would expect, the cost of underestimating the disease decreases. The planner views potential outcomes under the worst-case model to be far less adverse than they might have otherwise. As a result, the planner acts as if there is essentially no uncertainty about the impact of a new virus and chooses an optimal quarantine strategy accordingly. This key finding demonstrates that not only does choosing optimal policy under uncertainty lead to important increases in quarantine in the case that the virus has been underestimated, but also that excess economic costs from high levels of quarantine are now worse than when choosing optimal policy as if there was no uncertainty.

This paper links to a literature on robust control beginning with Hansen and Sargent (2001). Detailed explanations of robust preference problems and axiomatic treatment of such formulations using penalization methods are given by Anderson, Hansen, and Sargent (2000), Hansen, Sargent, Turmuhambetova, and Williams (2001), Cagetti, Hansen, Sargent, and Williams (2002), Anderson, Hansen, and Sargent (2003), Hansen, Sargent, Turmuhambetova, and Williams (2006), Maccheroni, Marinacci, and Rustichini (2006), and Hansen and Sargent (2011). The paper also relates to a literature on dealing with policy uncertainty, for example Bloom (2009) and Baker, Bloom, and Davis (2016).

We apply tools developed to the economic costs of climate change, given model uncertainty regarding the projected effects of climate change. Much research has focused on determining whether the impacts of climate change are temporary damages on the level of output, or more permanent damages on the growth rate of output (see Dell, Jones, and Olken (2012), Colacito, Hoffmann, and Phan (2018), Hsiang, Kopp, Jina, Rising, Delgado, Mohan, Rasmussen, Muir-Wood, Wilson, Oppenheimer, et al. (2017), Baldauf, Garlappi, and Yannelis (2019) and Burke, Davis, and Diffenbaugh (2018) for examples focused on empirically estimating these different types of climate damages). Level effects can lead to very different choices by social planners in terms of choices about emissions and carbon mitigation in a climate economic setting compared to growth effects (see Hambel, Kraft, and Schwartz (2015) and Barnett, Brock, and Hansen (2020) for theoretical examples showing how these different types of damages can lead to very different social costs of carbon results). However, in our pandemic setting the planner is able to use optimal policy to determine whether to subject the economy to quarantine measures that produce short-term damages or larger long-term damages that are partially discounted. This is the key effect driving the planner's optimal decision. The role that model uncertainty plays is amplifying concerns about the worst case outcomes, that infection and death rates are potentially much higher and thus the permanent effects could be much worse. As a result, the planner shifts more weight to the possibility of larger permanent, long-term costs coming from increased deaths and as a result increases current, short-term costs from quarantine measures in a dynamic model.

The paper introduces uncertainty to the discussion on economic responses to the COVID-19 epidemic. A number of studies have built macroeconomic frameworks, combining SIR models from epidemiology with macroeconomic models, such as Kaplan, Moll, and Violante (2020), Jones, Philippon, and Venkateswaran (2020), Baker, Bloom, Davis, and Terry (2020) and Eichenbaum, Rebelo, and Trabandt (2020). These studies rely on calibrated parameters, which are often unknown. Parameter uncertainty is widely noted in this literature, and authors typically use a range of values. For example, Acemoglu, Chernozhukov, Werning, and Whinston (2020) note that: *"We stress that there is much uncertainty about many of the key parameters for COVID19 (Manski and Molinari, 2020) and any optimal policy, whether uniform or not, will be highly sensitive to these parameters (e.g., Atkeson (2020a), Avery, Bossert, Clark, Ellison, and Ellison (2020), Stock (2020)). So our quantitative results are mainly illustrative and should be interpreted with caution."* Our paper offers a framework for incorporating uncertainty explicitly in a wide class of

macroeconomics models.

Other studies have studied the impact of the COVID-19 epidemic on household consumption (Baker, Farrokhnia, Meyer, Pagel, and Yannelis, 2020a,b), social distancing (Barrios and Hochberg, 2020, Allcott, Boxell, Conway, Gentzkow, Thaler, and Yang, 2020), labor markets (Coibion, Gorodnichenko, and Weber, 2020), small business Granja, Makridis, Yannelis, and Zwick (2020) and inequities (Coven and Gupta, 2020). Some papers also focus on estimating damages. Using historical data from the Spanish flu, Barro, Ursúa, and Weng (2020) argue for an upper bound of between 6 and 8 percent of GDP for the impact of the virus. Gormsen and Koijen (2020) argue that stock market reactions imply an approximate 2 to 3 percent change in GDP growth.

The remainder of this paper is organized as follows. Section 2 discusses uncertainty. Section 3 presents our model. Section 4 describes how to account for uncertainty. Section 5 presents simulation results. Section 6 discusses model extensions and section 7 concludes.

2 Uncertainty and Pandemics

We differentiate three aspects of uncertainty following Knight (1971) and Arrow (1951), and discuss how they are best understood in the context of an epidemic.

1. **Risk** refers to outcomes within a model where probabilities are known.[5] For example, by going to work, there is a risk that an individual catches the disease; once infected, there is a risk that the individual dies. These risks are present regardless of our knowledge of the parameters underlying the pandemic.

2. **Ambiguity**, refers to uncertainty across models, where, for example, a researcher or policy maker does not know how much weight to assign to one model as opposed to another. For example, from the perspective of a policymaker, a new disease may have a mild CFR or it may have a high CFR, and the policymaker does not know how much weight to assign one model versus another.

3. **Misspecification** or model uncertainty refers to uncertainty about models, or flaws in models not known to researchers. For example, from the perspective of a poli-

[5] A large literature refers to this risk as uncertainty, for example Bloom (2009) and Baker, Bloom, and Davis (2016). To avoid confusion, we use the terms risk to denote a situation where probabilities are known and ambiguity to refer to a situation where probabilities are unknown.

cymaker there is a range of plausible CFRs for a new disease, and the policymaker worries that the CFR used to form policy decisions may be misspecified.

In the context of COVID-19, there was significant uncertainty regarding its overall effects in early 2020 (Chater, 2020), relating to risk, ambiguity and misspecification. It is understood that it is risky to expose oneself to the disease, and at a high level, the SIR model captures important aspects of pandemic spread. However, whether a healthy person coming in contact with an infected person has a 1% or 10% chance of contracting the disease, and whether an infected person has a 0.1% or 10% chance of dying, is critical in shaping policy yet unknown to policymakers. Our approach in this paper is to explicitly model optimal policymaker decision rules under potential model misspecification, focusing on the CFR and $\mathcal{R}_0$ of the disease.

Figure 1: Estimated CFR Rates by Country

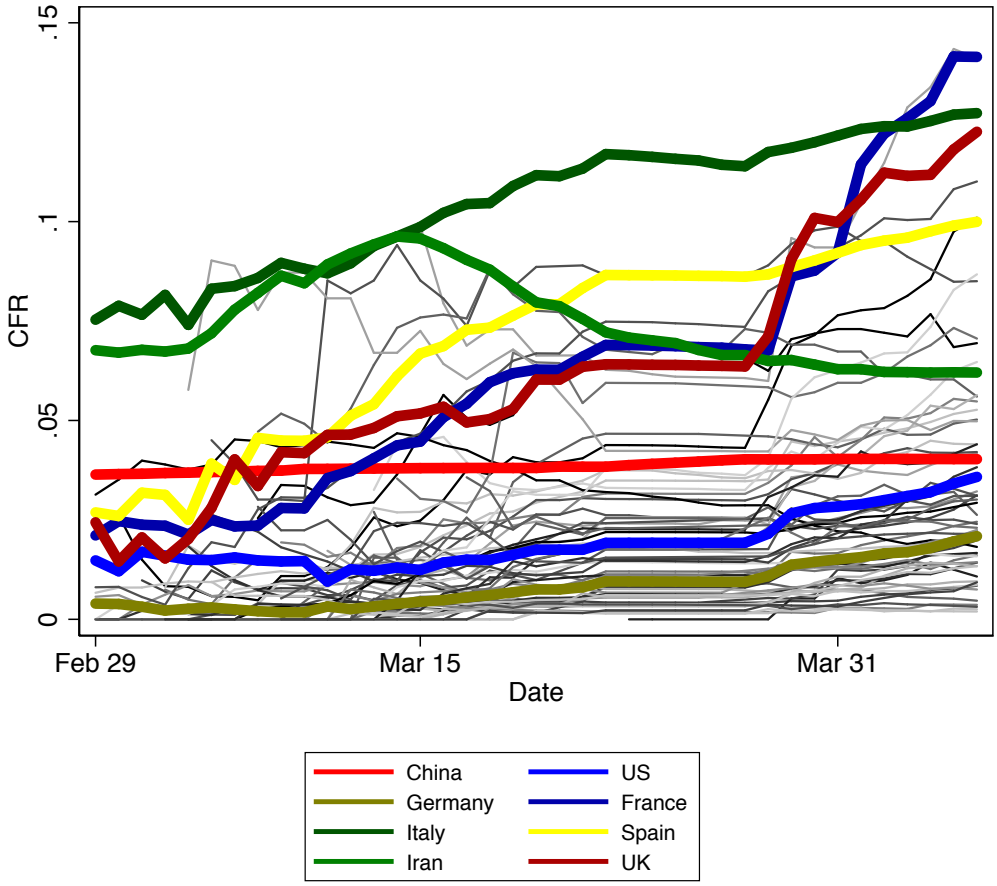

Notes: This figure shows estimated CFR rates for all countries with more than 1,000 cases and 100 deaths. Source: European Centre for Disease Prevention and Control.

First, there were significant differences in estimates of the CFR across countries. For example, in Italy the CFR as 12.67%, while in Germany the CFR was 2.07%– an approximate sixfold difference. Figure 1 shows CFR rates by country between March 1 and April 9, 2020 during the early spread of the pandemic in Europe and the United States. The eight countries with the largest number of COVID-19 cases at the time are highlighted. While several countries estimate CFR rates above 10%, some estimates put the CFR as being as low at .1%. Estimating a CFR for a new disease while cases are ongoing is inherently difficult, as cases must be closed through either recovery or death before a CFR can be computed (Spychalski, Błażyńska-Spychalska, and Kobiela, 2020). Additionally, many countries have very different reporting and testing practices, making it difficult to estimate the number of confirmed cases and deaths due to COVID-19 versus other causes.

Figure 2: Estimated $\mathcal{R}_0$ for Countries and States

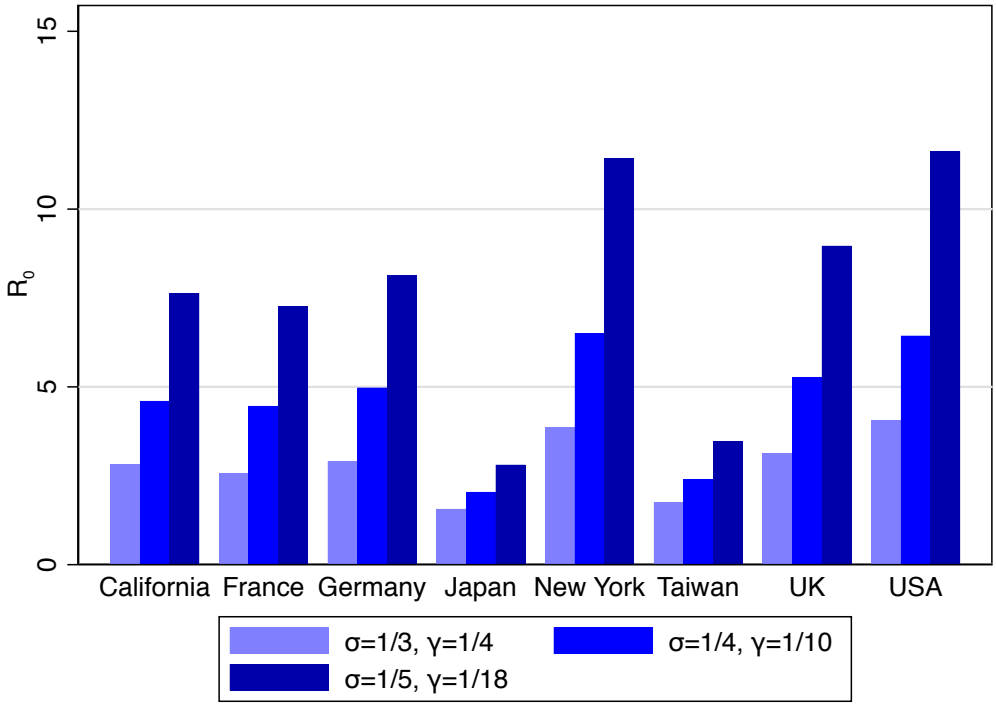

This figure shows estimated $\mathcal{R}_0$ rates for different countries and states, and different parameters of the incubation period of the disease (σ) and the estimated duration of the illness (γ). Source: Korolev (2020).

Second, estimates of the basic reproduction number, $\mathcal{R}_0$, varied widely. $\mathcal{R}_0$ is the expected number of new cases generated by a single case in an uninfected population and a key determinant of the spread of the disease. Estimates ranged from 1.5 to 12 (Korolev, 2020). A key threshhold is whether $\mathcal{R}_0 \lessgtr 1$: When $\mathcal{R}_0 > 1$, it means that the disease will spread in the population, because a single infected will spread it to multiple people, who will then spread it to multiple people, and so on. In contrast, an $\mathcal{R}_0 < 1$ means that the number of infected people will decrease over time because each infected person will infect less than one other and will herself eventually recover or die. Figure 2 shows estimates of the parameter in several states and countries, under different parameterizations of the incubation period of the illness and duration. This uncertainty about $\mathcal{R}_0$ is noted in many academic papers, for example Stock (2020) notes in a paper on data gaps related to COVID-19 that "*A key parameter, the asymptomatic rate (the fraction of the infected that are not tested under current guidelines), is not well estimated in the literature because tests for the coronavirus have been targeted at the sick and vulnerable.*"

One key factor regarding uncertainty in both the CFR and $\mathcal{R}_0$ was a lack of testing, and the fact that many cases are initially asymptomatic. This makes it very difficult to ascertain the true number of individuals infected with COVID-19, and hence determine the CFR and $\mathcal{R}_0$. Many policymakers and academics were well aware of uncertainty surrounding key determinants of the health costs of COVID-19. For example, the Asian Development Bank cited a range of parameters of $\mathcal{R}_0$ between 1.5 and 3.5, and a CFR between 1% and 3.4%, and notes that these are imprecisely estimated.

In the subsequent analysis, we focus on uncertainty about these two parameters.[6] To do so, we first present a simple economic model of an epidemic without uncertainty. Here, the central planner has full knowledge of the virus's $\mathcal{R}_0$ and CFR, and chooses an optimal quarantine policy taking into account its future impact on the spread of the virus as well as the economic costs of quarantine. We then add parameter uncertainty by augmenting the social planner decision problem using either a smooth ambiguity approach or a robustness approach to explore how parameter uncertainty impacts the optimal policy.

[6]It is important to note that there are also other potential, un-modeled health costs. For example, even if the CFR is low, COVID-19 could cause permanent damage to lungs in a fashion similar to SARS, a related coronavirus. Additionally, in follow-on work we plan to incorporate uncertainty about the economic costs of mitigation measures.

3 A Simple Economic Model of an Epidemic

We first sketch out a simple economic model of an epidemic without model uncertainty. We then explicitly incorporate model uncertainty in subsequent sections. Our model begins with a standard Susceptible-Infectious-Recovered (SIR) framework used throughout mathematics, medicine, epidemiology, and other fields that study pandemics.[7] We augment this SIR model with an economic model that allows us to speak to the costs of the disease as well as the costs and benefits of mitigation efforts.

3.1 Epidemic Model

A standard SIR model is characterized by three states: the fraction of the population that is susceptible to the disease, s_t, the fraction of the population infected by the disease, i_t, and the fraction of the population recovered from infection, r_t. We include a fourth state, death, d_t, which tracks the fraction of the population that has died because of the disease. The size of the population is assumed to be fixed. These states evolve as follows:

$$\begin{aligned} ds_t &= -\beta s_t i_t dt \\ di_t &= \beta s_t i_t dt - (\rho + \delta) i_t dt \\ dr_t &= \rho i_t dt \\ dd_t &= \delta i_t dt \end{aligned}$$

β is the rate at which a susceptible becomes infected when meeting a an infected. ρ is the rate at which an infected recovers, and δ is the rate at which an infected dies.

We allow for uncertainty about the SIR model parameters. The key parameters we focus on are $\mathcal{R}_0$, the expected number of secondary cases that a single infection produces in a fully-susceptible population, and the case fatality rate (CFR), which is the proportion of deaths relative to the total number of infected. These two parameters, combined with the expected duration of the disease (γ), link to the key structural disease parameters in our model, β, ρ, and δ, as follows:

$$\mathcal{R}_0 = \frac{\beta}{\gamma}, \quad CFR = \frac{\delta}{\gamma}, \quad \gamma = \rho + \delta$$

We allow for uncertainty connected to these two parameters in our model in multiple

[7] Stanford Earth System Sciences notes provide a basic outline of a standard epidemiological SIR model.

ways. First, we introduce Brownian shocks connected to the evolution of i_t and d_t to the deterministic transition rates above. These shocks capture, among other things, variability in exposures, variability in the co-morbidities of the affected population, and potential mismeasurement of the number of infected and dead.

These shocks are critical when we later add parameter uncertainty, because they prevent policy makers from immediately learning about the fundamental transition rates of the disease. We add these shocks under a few key assumptions: the first shock is perfectly negatively correlated between s_t and i_t so that shocks to infections only occur in the susceptible population, which one can interpret as uncertainty over whether an individual is infected or has never been infected; the second shock is perfectly negatively correlated between i_t and d_t so that shocks to deaths occur in the infected population; and all shocks are scaled by i_t so that when there are no infected individuals there can no longer be shocks to the number of infected and dead. With these shocks and assumptions, the state variable evolution becomes:

$$
\begin{aligned}
ds_t &= -\beta s_t i_t dt - \sigma_\beta i_t dW_i \\
di_t &= \beta s_t i_t dt - (\rho + \delta) i_t dt + \sigma_\beta i_t dW_i - \sigma_\delta i_t dW_d \\
dr_t &= \rho i_t dt \\
dd_t &= \delta i_t dt + \sigma_\delta i_t dW_d
\end{aligned}
$$

Formally, $W \doteq \{W_t : t \geqslant 0\}$ is a multi-dimensional Brownian motion where the corresponding Brownian filtration is denoted by $\mathcal{F} \doteq \{\mathcal{F}_t : t \geqslant 0\}$ and $\mathcal{F}_t$ is generated by the Brownian motion between dates zero and t. Figure 3 illustrates the transition rates between states in our model under this risk based framework.

Including Brownian shocks in our model captures the risk channel of uncertainty. However, key to our analysis will be extending our analysis to account for additional channels of uncertainty. In our analysis, we will explore the impact of he ambiguity-based channel of uncertainty and the misspecification-based channel of uncertainty, which we explicitly model in later sections of the paper.

Figure 3: Transition Rates between States in the Augmented SIR Model.

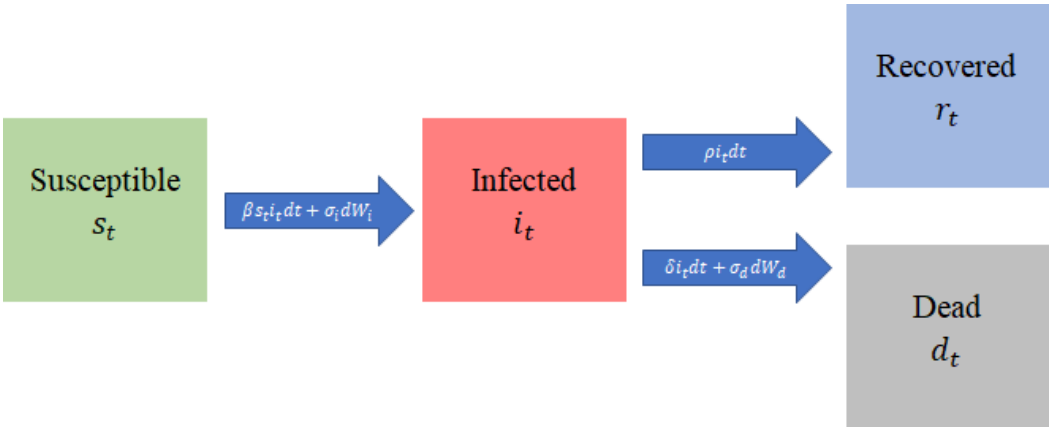

3.1.1 Pandemic Mitigation

We allow for pandemic mitigation through quarantine measures. Let q_t be the fraction of the population in quarantine at any period of time.[8] Quarantine prevents susceptible individuals from contracting the virus and becoming infected. Given the mitigation policy q_t, the law of motions for the susceptible and infected populations become:

$$ds_t = -\beta(s_t - q_t)i_t dt - \sigma_\beta i_t dW_t$$
$$di_t = \beta(s_t - q_t)i_t dt - (\rho + \delta)i_t dt + \sigma_\beta i_t dW_t - \sigma_\delta i_t dW_t$$

3.2 Economic and Public Health Model

Household (flow) utility depends on households' level of consumption C_t, given by

$$U = \kappa \log C_t$$

The level of consumption will depend on production and the public health costs and consequences resulting from the pandemic, which we detail below.

3.2.1 Production and Consumption

We assume a linear production technology for the consumption good with labor being the only input. Public health costs from infections and deaths reduced the amount of output

[8] We refer to the policy mitigation as "quarantine," but the parameter q_t captures a wide range of policies such as school closures, business closures and shelter-in-place orders.

that can be consumed. Households consume everything that is produced:

$$C_t = Y_t = AL_t$$

C is consumption, Y is output, A is labor productivity (including the capital stock, which we hold fixed for this exercise), L is the labor supply in the economy. We assume that labor is supplied perfectly inelastically, but due to the pandemic, the supply of labor may shrink as workers become ill, die, or are quarantined. In particular, letting $\bar{L}$ represent the non-pandemic labor supply, we assume that

$$L_t = \bar{L}(s_t + r_t - aq_t^b)$$

That is, only the susceptible and recovered populations can supply labor or consume. Observe that this builds in the public health costs of the pandemic: The public health cost of an infected worker is that she cannot work or consume and foregoes her flow consumption utility until she recovers. The public health cost of a dead worker is the total present utility value of her future production and consumption that is permanently foregone. In extensions to the model, we will consider modeling additional public health costs, such as the costs of an overloaded medical system or the emotional anguish and suffering caused by the disease.

Additionally, we assume that the quarantine policy reduces the available labor supply by aq_t^b, with $a > 0$ and $b \geqslant 1$. This potentially convex functional form captures the idea that for very mild quarantine measures, workers who can most productively work from home will do so, thereby not greatly reducing the effective labor supply. As quarantine measures become more strict, more essential workers are forced into quarantine and effective labor units are reduced at an increasing rate. Hence, the consumption-equivalent per-worker economic cost of quarantine measures is aAq_t^b.

4 Model Solutions

We now derive the solution to the model for three settings: (1) the model solution without uncertainty; (2) the model solution adjusted for concerns about ambiguity-based model uncertainty; and (3) the model solution adjusted for concerns about misspecification-based model uncertainty. The solution to the model without uncertainty is the standard framework used throughout much of the economics and finance literature to understand how optimal choices are made based on known models and distributions. Because of the stochastic

nature of the model, we consider this a "risk-based" uncertainty setting. In our numerical results, we will show how solutions of this form vary based on parameter sensitivity analysis, which has been called "outside the model" uncertainty, showing how different assumptions about the model parameters change the optimal outcomes, but the social planner does not account for this when making optimal policy choices.

The two remaining model solutions are "ambiguity-based" and "misspecification-based" uncertainty settings that show how optimal policy decisions and model solutions differ when the social planner incorporates concerns about uncertainty into their decision problem. This type of uncertainty analysis is sometimes called "inside the model" uncertainty, and will build on the continuous-time smooth ambiguity framework developed in Hansen and Sargent (2011) and Hansen and Miao (2018), and the continuous-time robustness framework developed in Anderson et al. (2003), Hansen et al. (2006), Maccheroni et al. (2006), and others. One key assumption to note that we apply throughout our analysis is that we abstract from any form of Bayesian learning or updating in the model. Given the rapid development of the COVID-19 pandemic and the extreme difficulty in determining the true model for policymakers responding in real-time to the pandemic, we view this assumption as a reasonable starting point.

As we will be solving an infinitely-lived representative agent's problem, and with the adding up constraint of $1 = s_t + i_t + r_t + d_t$ and the remaining structure of the problem, our solution will be defined by a recursive Markov equilibrium, where optimal decisions and the value function are dependent only on the current value of the state variables s_t, i_t, d_t. The equilibrium definition is given by an optimal choice of mitigation $\{q_t\}$, which is a function of state variables s_t, i_t, d_t, such that

1. Households maximize lifetime expected utility
2. The household budget constraint holds
3. The firm maximizes discounted, expected lifetime profits
4. Goods and labor market clearing hold

Each of the following solutions will follow this equilibrium concept, with adjustments made based on whether the agent incorporates uncertainty into their decision problem and the type of uncertainty adjustment they use in their decision problem.

4.1 Optimal Policy Without Uncertainty

We start our analysis by examining the socially optimal framework without uncertainty about COVID-19. We also shut down additional public health costs beyond the consumption-equivalent economic cost of quarantine measures to highlight the key mechanisms and intuition, which will then allow us to understand the role additional features will play, in particular model uncertainty.

The household or social planner problem is to maximize lifetime expected utility by choosing the optimal mitigation or quarantine policy q_t. This problem is given by

$$V(s_t, i_t, d_t) = \max_{q_t} E_0[\int_0^\infty \log(C_t)dt]$$

subject to market clearing and labor supply and budget constraints.

We focus on solving for the social planner's problem, which can be represented using a Hamilton-Jacobi-Bellman (HJB) equation for the value function resulting from the household or social planner's optimization problem[9], by

$$\begin{aligned} 0 = -\kappa V + \kappa \log[AL(1 - i_t - d_t - q_t)] \\ +V_s[-\beta(s_t - q_t)i_t] + V_i[\beta(s_t - q_t)i_t - (\rho + \delta)i_t] + V_d[\delta i_t] \\ +\frac{1}{2}\{V_{ss}\sigma_\beta^2 + V_{ii}[\sigma_\beta^2 + \sigma_\delta^2] + V_{dd}\sigma_\delta^2\}i^2 \\ -\{\sigma_\beta^2 V_{si} + \sigma_\delta^2 V_{id}\}i^2 \end{aligned}$$

The optimal choice of mitigation q_t is the solution to a quadratic equation resulting from the first-order condition and is given by

$$q_t = \frac{-(\kappa a) \pm \sqrt{(\kappa a)^2 + a(V_s - V_i)^2(\beta i_t)^2(1 - i - d)}}{a(V_s - V_i)(\beta i_t)}$$

The optimal choice of mitigation is thus a function of parameters such as β, the rate at which a susceptible becomes infected when meeting an infected, as well as the value function derivatives or the marginal value of increases in the infected and susceptible populations. We next explore how the social planner should respond when parameters are unknown.

[9]Details on derivation of the HJB equations can be provided upon request.

4.2 Optimal Policy With Uncertainty — Smooth Ambiguity

The first way we will account for model uncertainty is by applying the smooth ambiguity methodology established in the economics literature.[10] Accounting for uncertainty in this way allows the social planner to make optimal mitigation policy choices while acknowledging that the true distribution for the set of models under consideration is ambiguously specified or unknown. We will exploit the mathematical tractability of the continuous-time smooth ambiguity decision problem to characterize the implications of uncertainty for optimal policy decisions in an intuitive way based on a discrete set of potential models. Our description of how smooth ambiguity alters the social planner's decision problem will be concise. We also explore a second way for accounting for model uncertainty by applying the robust preferences methodology established in the economics literature, which we discuss later in the section on model extensions and give results for in the appendix.

We begin by assuming that there is a discrete set Υ of possible models υ for the pandemic. For each $\upsilon \in \Upsilon$ there is a set of parameters $\beta(\upsilon), \rho(\upsilon), \delta(\upsilon)$ which characterize the state variable evolution equations as follows:

$$
\begin{aligned}
ds_t &= -\beta(\upsilon)(s_t - q_t)i_t dt - \sigma_\beta i_t dW_t \\
di_t &= \beta(\upsilon)(s_t - q_t)i_t dt - (\rho(\upsilon) + \delta(\upsilon))i_t dt + \sigma_\beta i_t dW_t - \sigma_\delta i_t dW_t \\
dd_t &= \delta(\upsilon)i_t dt + \sigma_\delta i_t dW_t
\end{aligned}
$$

Each of these υ conditional models is assumed to come from existing estimates of the model either from historical data of previous viral pandemics or from real-time estimates from different outbreaks and acts as a potential best-guess for what the true pandemic model is for policymakers. The social planner in our model will make optimal policy decisions conditional on each model, and then allow for the fact that the distribution for the set of models is ambiguously specified or unknown and will then adjust their optimal policy decision in response to the pandemic accordingly.

To avoid additional complexities and complications, we will assume that there is no uncertainty about volatilities given for the model. Under this assumption, we can avoid any concerns that uncertainty about the true model can be revealed immediately from observed

[10] Axiomatic treatment, complete mathematical details, and applications of smooth ambiguity problems are given by Gilboa et al. (1989), Chen and Epstein (2002), Klibanoff et al. (2005), Hansen and Sargent (2007), Hansen and Sargent (2011), Hansen and Miao (2018), Hansen and Sargent (2019), and Barnett et al. (2020).

outcomes. Though the analysis can be extended to such settings under proper conditions, this assumption allows us to carry out a revealing analysis of the impact of uncertainty under the smooth-ambiguity based decision theoretic framework in a straightforward manner.

For each υ conditional model the social planner solves a conditional problem maximizing lifetime expected utility by choosing the optimal mitigation or quarantine policy $q_t(\upsilon)$ conditional on the given υ model. This conditional problem is given by

$$V(s_t, i_t, d_t; \upsilon) = \max_{q_t(\upsilon)} E_0[\int_0^\infty \log(C_t(\upsilon))dt|\upsilon]$$

subject to market clearing and labor supply and budget constraints.

We can represent the solution for the value function $V(\upsilon)$ using a Hamilton-Jacobi-Bellman (HJB) equation resulting from the household or social planner optimization problem, which is given by

$$\begin{aligned} 0 = -\kappa V(\upsilon) + \kappa \log[AL(1 - i_t - d_t - q_t(\upsilon))] \\ +V_s(\upsilon)[-\beta(\upsilon)(s_t - q_t(\upsilon))i_t] + V_i[\beta(\upsilon)(s_t - q_t(\upsilon))i_t - (\rho(\upsilon) + \delta(\upsilon))i_t] + V_d(\upsilon)[\delta(\upsilon)i_t] \\ +\frac{1}{2}\{V_{ss}(\upsilon)\sigma_\beta^2 + V_{ii}(\upsilon)[\sigma_\beta^2 + \sigma_\delta^2] + V_{dd}(\upsilon)\sigma_\delta^2\}i^2 \\ -\{\sigma_\beta^2 V_{si}(\upsilon) + \sigma_\delta^2 V_{id}(\upsilon)\}i^2 \end{aligned}$$

The optimal choice of mitigation $q_t(\upsilon)$ is the solution to a quadratic equation resulting from the first-order condition and is given by

$$q_t(\upsilon) = \frac{-(\kappa a) \pm \sqrt{(\kappa a)^2 + a(V_s(\upsilon) - V_i(\upsilon))^2(\beta(\upsilon)i_t)^2(1 - i - d)}}{a(V_s(\upsilon) - V_i(\upsilon))(\beta(\upsilon)i_t)}$$

The optimal choice of mitigation is now a function of the conditional model parameters $\beta(\upsilon)$, and the conditional marginal values of changes to the susceptible and infected populations, represented by $V_s(\upsilon), V_i(\upsilon)$.

To incorporate uncertainty, we will now apply the decision theoretic framework developed in Hansen and Sargent (2011) and Hansen and Miao (2018). We first specify a prior distribution to the set of models $\upsilon \in \Upsilon$, by assigning a probability weight $\pi(\upsilon)$ to each model υ. Note that for these weights to be well defined as probability weights they must satisfy the following conditions:

$$\pi(\upsilon) \geqslant 0, \quad \forall \upsilon$$

$$\sum_{\upsilon \in \Upsilon} \pi(\upsilon) = 1.$$

Like the alternative models in our set, the prior probability weights are assumed to come from historical data or real-time observational inference.

We then allow for uncertainty aversion by using a penalization framework based on conditional relative entropy. This framework allows the planner to consider alternative distributions or sets of weights $\tilde{\pi}(\upsilon)$ across the set of conditional models in a way that is statistically reasonable by restricting the set of alternative models considered by the social planner to those that are difficult to distinguish from the prior model distribution using statistical methods and past data.[11] The parameter θ_a is chosen to determine the magnitude of this penalization. Relative entropy is defined as the expected value of the log-likelihood ratio between two models or the expected value of the log of the Radon-Nikodym derivative of the perturbed model with respect to approximating one. The value of relative entropy is weakly positive, and zero only when the models are the same.[12]

This new, second-stage problem for the planner is a minimization problem, where the minimization is made over possible distorted probability weights $\tilde{\pi}(\upsilon)$ which are constrained by θ_a based on the solutions to the υ conditional value function solutions found previously. This allows the planner to determine the relevant worst-case model for given states of the world to help inform their optimal policy decisions. Though optimal decisions will be determined by considering alternative worst-case models, this setting should not be interpreted as a distorted beliefs model. The worst-case model is used as a device to produce solutions that are robust to alternative models. The second-stage minimization problem is given by the solution to the following problem

$$\hat{V}_t = \min_{\tilde{\pi}(\upsilon)} \sum \tilde{\pi(\upsilon)}(V(\upsilon) + \theta_a[\log(\tilde{\pi}(\upsilon)) - \log(\pi(\upsilon))])$$

[11] To give a concrete example in the context of COVID-19, it may be relatively easy to observe the number of people who died from the pandemic but difficult to observe the number of people who were infected. On the basis of this data, it is difficult to tell whether the disease has a very high spread rate ($\mathcal{R}_0$) and a low death rate (CFR), or a low spread rate and a very high death rate, yet the optimal response is likely to be very different under these scenarios.

[12] See Hansen and Sargent (2011) for details about relative entropy in this setting. Using relative entropy means we are only considering relatively small distortions from the baseline model, but even small distortions can have significant impacts on optimal policy. In particular, we apply relative entropy penalization directly to the set of conditional value functions. We could instead apply relative entropy penalization to the stochastic increments of the model, which would require that we scale relative entropy linearly by dt and solve a single, non-linearly adjusted HJB equation, but we find the current framework tractable and appealing for comparison with the outside the model sensitivity analysis we will conduct later on.

$$\text{subject to} \sum \pi(\upsilon) = \sum \tilde{\pi}(\upsilon) = 1$$

Taking the first order condition for this problem, and imposing the constraint $\sum \tilde{\pi}(\upsilon) = 1$, we can solve for the optimally distorted probability weights, which are given by

$$\tilde{\pi}(\upsilon) = \frac{\pi(\upsilon) \exp(-\frac{1}{\theta} V(\upsilon))}{\sum \pi(\upsilon) \exp(-\frac{1}{\theta_a} V(\upsilon))}$$

As the $\tilde{\pi}(\upsilon)$ in the model are optimally determined and state dependent, the magnitude of the ambiguity considered by the social planner when making optimal policy decisions will depend on the current state of the pandemic and evolve dynamically. Plugging the optimally distorted probability weights back into the optimization problem provides us with the optimized value function under smooth ambiguity

$$\hat{V}_t = -\theta \log[\sum \pi(\upsilon) \exp(-\frac{1}{\theta_a} V(\upsilon))]$$

For both the distorted probability weights and the optimized value function under uncertainty, we see that smooth ambiguity plays the role of imposing an exponential tilting towards those υ conditional models that lead to the most negative lifetime expected utility implications. A smaller value of θ_a enhances the magnitude of the concern about ambiguity, and the prior probability weights play an important role for anchoring the outcomes to a baseline expectation of the true model. In order to determine the ambiguity robust policy for the social planner, we weight the υ conditional optimal mitigation policies $q_t(\upsilon)$ using the distorted probability weights to get

$$\tilde{q}_t = \sum_{\upsilon} \tilde{\pi}(\upsilon) q_t(\upsilon)$$

The exponential tilting of the distorted probability weights carries through to our determination of the optimal mitigation strategy. The magnitude with which we weight each υ conditional model informs us how to weight the υ conditional mitigation policy as well. Finally, this same reweighting by the distorted probability weights provides us with the distorted parameters which the social planner uses to make optimal policy decisions in this setting, which are given by

$$\hat{\beta}_t = \sum_{\upsilon} \tilde{\pi}(\upsilon) \beta(\upsilon)$$

$$\hat{\delta}_t = \sum_{\upsilon} \tilde{\pi}(\upsilon)\delta(\upsilon)$$

As the planner tilts their value function and probability weights towards certain models, this leads to the implied distorted model parameters which are informed by worst-case outcomes which the planner uses as a lens to view and respond in a robustly optimal way in the face of uncertainty.

5 Numerical Results

We will now provide numerical results from simulations based on the theoretical solutions provided above. We will first show results based on the set of model solutions solved assuming no uncertainty in an "outside the model" sensitivity analysis. These results show the dispersion in possible model outcomes even when the planner does not account for uncertainty and indicate the importance of accounting for uncertainty by the social planner. We will then show the role of "inside the model" uncertainty using three different scenarios: (i) when the social planner has underestimated the pandemic; (ii) when the social planner has correctly guessed the true model for the pandemic; and (iii) when the social planner has overestimated the pandemic. For each scenario we will show the outcomes assuming the planner knows the true model, the outcomes based on the assumed prior but not accounting for model uncertainty, and the outcomes based on the assumed prior but accounting for model uncertainty. We focus our "inside the model" uncertainty numerical results on the smooth ambiguity solution for two reasons. First, while the robustness setting has distinct and important features to consider, the numerical results (which we provide in the appendix) turn out to be quite similar to the smooth ambiguity results. Second, the smooth ambiguity setting allows us to explore how the social planner weighs the set of possible models in making optimal decisions, a particularly valuable and revealing result that will provide intuition for the observed results in our numerical analysis.

5.1 Calibration

There are a number of economic and pandemic related parameters that we choose values for that we discuss now. For the economic side of the model, we assume a working population of 164 million, consistent with the total US labor supply, and that per worker weekly output is given by $\$2,345$ so that output in the non-pandemic version of the model ($A \times L$) matches

recent, pre-pandemic data on weekly US GDP of $384 billion dollars. We choose an annual discount rate of 2%, and so the subjective discount rate κ, the weekly counterpart to this value, is given by $\kappa = 0.000384$. For the baseline analysis, we assume a convex quarantine cost structure where $a = 1.25$ and $b = 2$.

For the pandemic model parameters, we use values from various studies (including Korolev (2020), Atkeson (2020b), Atkeson (2020a), Wang et al. (2020), and estimates fromm the European Centre for Disease Prevention and Control) to set the expected time infected γ, the case fatality rate CFR, and the birth rate $\mathcal{R}_0$, which allows us to pin down the infection rate β, the death rate δ, and the recovery rate ρ. The value of γ is held fixed at $\gamma = \frac{7}{18}$. The set of underlying models used in our analysis use values of CFR in the set $\{0.005, 0.02, 0.035\}$ and values of $\mathcal{R}_0$ in the set $\{2.0, 3.5, 5.0\}$. These values are well within the range of values across these different studies. For the volatilities σ_β and σ_δ, we use data from the Center for Systems Science and Engineering in the Whiting School of Engineering at Johns Hopkins University[13] to calculate empirical counterparts for these values.

Finally, we must also specify values for the uncertainty parameters in our model, θ_a for smooth ambiguity and θ_m for robust preferences. Our values of θ_m and θ_m impose significant amounts of uncertainty aversion to demonstrate the potential magnitude of uncertainty impacts. The values we use are $\theta_a = 0.00004$ and $\theta_m = 0.0067$. These values can be difficult to interpret on their own, and are best interpreted by way of the conditional relative entropy values implied by these parameter choices and statistical discrimination bounds related to these conditional relative entropy values. In the model extensions section we discuss methods we will use to help discipline and calibrate our uncertainty parameter choices going forward based on these two criteria and from anecdotal evidence on model spreads implied by the recent estimates of COVID-19 parameter values.

5.2 Model Simulations

5.3 Outside the Model Uncertainty Through Sensitivity Analysis

We first provide simulated outcomes of the model based on different pandemic models without the planner accounting for uncertainty in their optimal decision. This corresponds to what is typically termed as a sensitivity analysis. It serves to illustrate the wide range of optimal responses and outcomes that depend on the underlying model parameters. This by itself is not a rigorous robust optimal control approach to model uncertainty. What

[13]This data is available through the CSSE GitHub repo.

the robust optimal control frameworks will provide are frameworks for the policymaker to optimally choose a *single* policy, simultaneously taking into account the variation in optimal responses across different pandemic models.

Figure 4 shows the spread of outcomes for s_t, i_t, r_t, d_t, and q_t across the different model cases. This is what is sometimes called "outside the model" uncertainty, or uncertainty in outcomes without accounting for how the decision makers choices are impacted by the uncertainty. The spreads are across all model outcomes for $\mathcal{R}_0 \in \{2, 3.5, 5\}$ and CFR $\in \{0.005, 0.02, 0.035\}$. Figure 4 indicates very different outcomes for s, i, r, d, and q, depending on model cases. The fact that outcomes change so drastically is suggestive that uncertainty about parameters may have important effects on optimal policy. Observe that across the models, the fraction of the dead population after 104 weeks varies by an order of magnitude, from less than 0.5% to nearly 2.5%. More strikingly, these are the death rates obtained by a policy maker that knows the true parameters and is reacting optimally, and in that sense provides a best-case outcome under each scenario.

Figure 4: Outside the Model Uncertainty

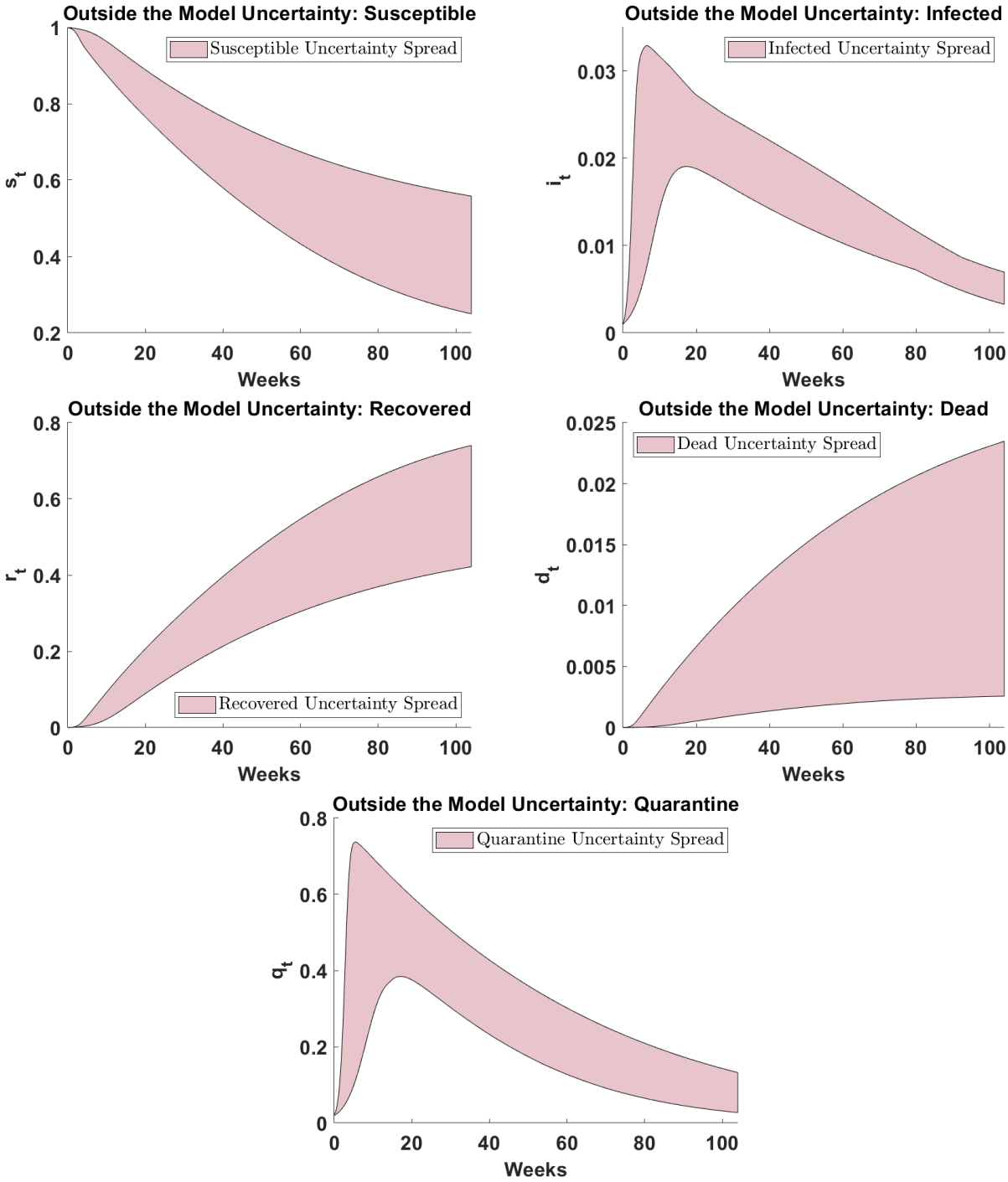

Notes: These figures show the range of possible outcomes and policy responses across nine potential models of the pandemic that vary by their $\mathcal{R}_0$ and CFR. From left to right, top to bottom, we show the fraction of the population that is susceptible, the fraction of the population that is infected, the fraction of the population that has had the disease and recovered, the fraction of the population that has died, and the fraction of the population under quarantine. We show the maximum and minimum for these variables across each model.

Figure 5: Outside the Model Uncertainty

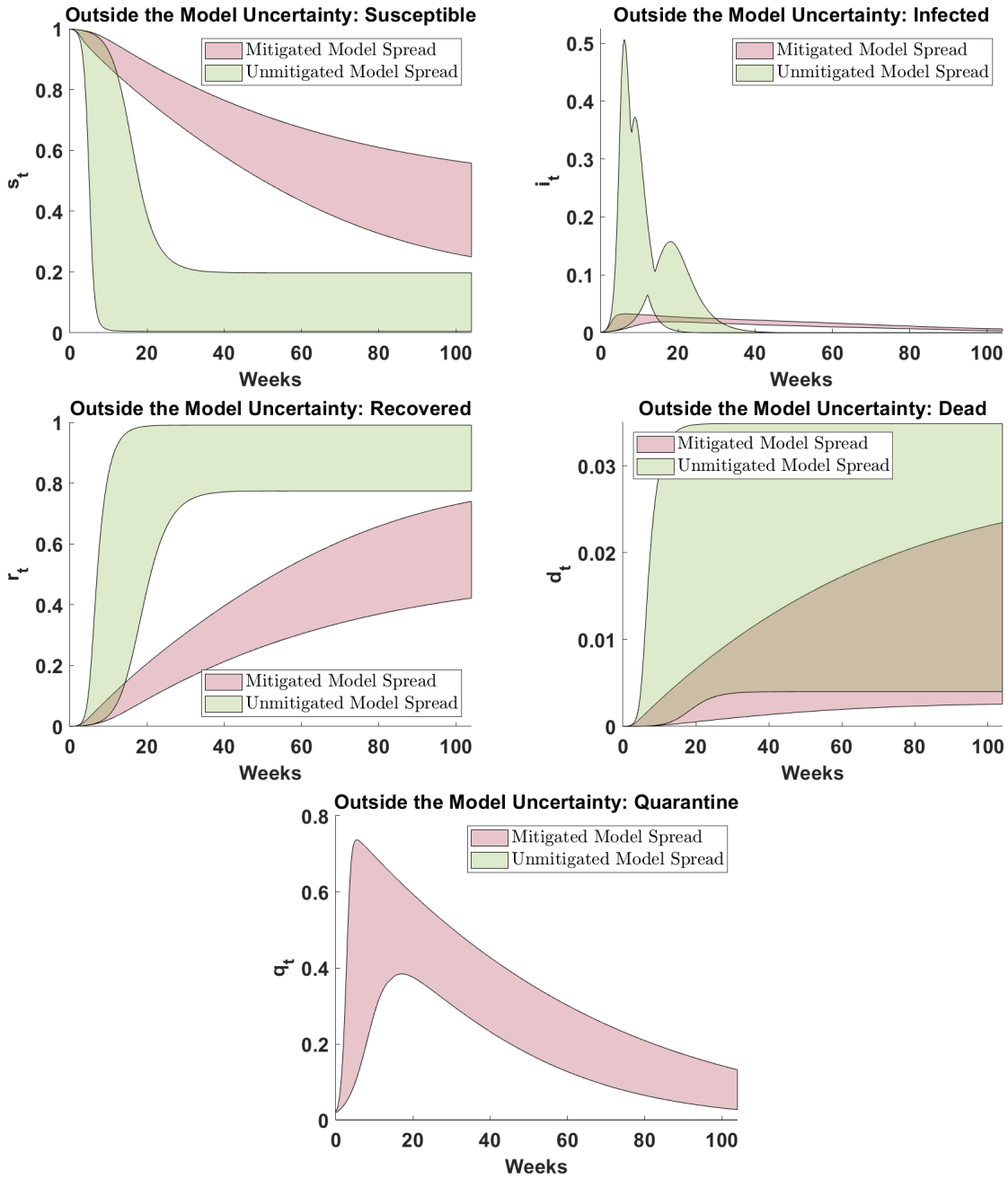

Notes: These figures show the range of possible outcomes and policy responses across models of the pandemic that vary by their $\mathcal{R}_0$ and CFR by the optimal quarantine policy. From left to right, top to bottom, we show the fraction that is susceptible, the fraction that is infected, the fraction that has had the disease and recovered, the fraction that has died, and the fraction under quarantine. The green shaded region shows spread of the simulated outcomes without any mitigation and the red shaded region shows the spread of the simulated outcomes with optimal mitigation. We show the maximum and minimum across each model.

Figure 5 augments our outside the model uncertainty comparison by adding to Figure 4 the spread of s_t, i_t, r_t and d_t across the different model cases if $q_t = 0$. Again these plots use the model specifications with combinations of $\mathcal{R}_0 \in \{2, 3.5, 5\}$ and CFR $\in \{0.005, 0.02, 0.035\}$. This figure not only demonstrates how critical mitigation and quarantine measures are in controlling a pandemic, but how much wider the spread can be if the planner does not take optimal policy action. The magnitude of pandemic impacts vary drastically depending on which model is the true underlying pandemic model, with some cases featuring much more rapid realization of the pandemic impacts and the number of dead and infected dramatically higher. Observe that across the models without quarantine, the fraction of the dead population after 104 weeks varies even more, from less than 0.5% to almost 3.5%. Furthermore, of the three peaks for infections, based on the three different $\mathcal{R}_0$ values, the worst reaches nearly 50%. These results further highlight the significant importance of quarantine measures and how severe a pandemic outbreak can be if the social planner making optimal policy has to respond without knowing the true model.

5.4 Inside the Model Uncertainty Through Smooth Ambiguity

Conditional on each model, the social planner's problem trades off short-term mitigation costs with long-term pandemic-related death and illness costs, and the need for a longer-lasting quarantine. More severe initial quarantine measures reduce the spread of the pandemic at the cost of current temporary reductions in the labor supply, and therefore production and consumption. However, less severe quarantine measures lead to increased deaths, which permanently reduce the labor supply, production, and consumption. As a result, even a small reduction in the number of deaths has a significant economic benefit, even without accounting for the first-order non-monetary losses from losing loved ones. Time discounting plays an important role, however, because the costs associated with quarantine are borne immediately, while longer-term costs are realized in the future. In consequence, immediately stopping all infections and deaths is also suboptimal. In short, regardless of the underlying model and uncertainty among them, the social planner faces a non-trivial tradeoff in enacting pandemic mitigation policies, but how this tradeoff should be optimally balanced varies substantially across models.

As we previously highlighted, the spread on estimates for $\mathcal{R}_0$ and CFR from numerous studies is substantial, and so understanding how policymakers can optimally respond in the face of such uncertainty is particularly relevant for this, or any other, economic and

public health crisis. The infection rate β and death rate δ are the parameters in our model we will focus on for understanding uncertainty, given their explicit connection to the CFR and $\mathcal{R}_0$ and the significant uncertainty that exists about these parameters. Once we introduce uncertainty, the worst-case outcomes are amplified. In this setting, the worst-case concerns are that infection and death rates are potentially higher and thus the permanent effects could possibly be much worse. In response, the planner shifts more weight to the possibility of experiencing larger permanent, long-term costs in terms of increased deaths because of the pandemic. As a result, at a high level, the social planner making optimal decisions under model uncertainty will tend to increases current, short-term costs from strengthening quarantine measures in a dynamic way to address these concerns.

The starting point for this analysis is the policy maker's prior over the models, $\pi(\upsilon)$, where υ is one of the possible models under consideration. We consider three scenarios, where, relative to the true parameters, the policy maker's prior (i) underestimates the pandemic (ii) correctly estimates the pandemic and (iii) overestimates the pandemic. We find through our analysis important asymmetries in policy responses across these different scenarios. Broadly, the effect of incorporating uncertainty in decision making has little effect when models correctly or overestimate the severity of a pandemic, limiting excess economic costs from quarantine measures. However, in a situation where the severity of the pandemic is initially underestimated and the disease is allowed to spread, incorporating uncertainty moves policy significantly towards what the optimal policy response would be had the social planner known the true underlying model.

We discuss these effects in detail, which are presented in Figures 6-10. In each figure, we show the state variables and optimal policy responses in three series. We show (i) the prior model response, which is the optimal response based on the policymaker's assumed prior distribution of probability weights across all models in consideration given the current state of the world, representing what one might consider to be a "naive" approach to model uncertainty where the policymaker acknowledges different potential models and adopts a fixed distribution; (ii) is the true optimal response had the policy maker known the true model; (iii) is the uncertainty adjusted response, where the policymaker optimally weighs each model to arrive at her decision that is designed to be robust to possible model uncertainty.

Figure 6: Scenario 1: Underestimating the Pandemic

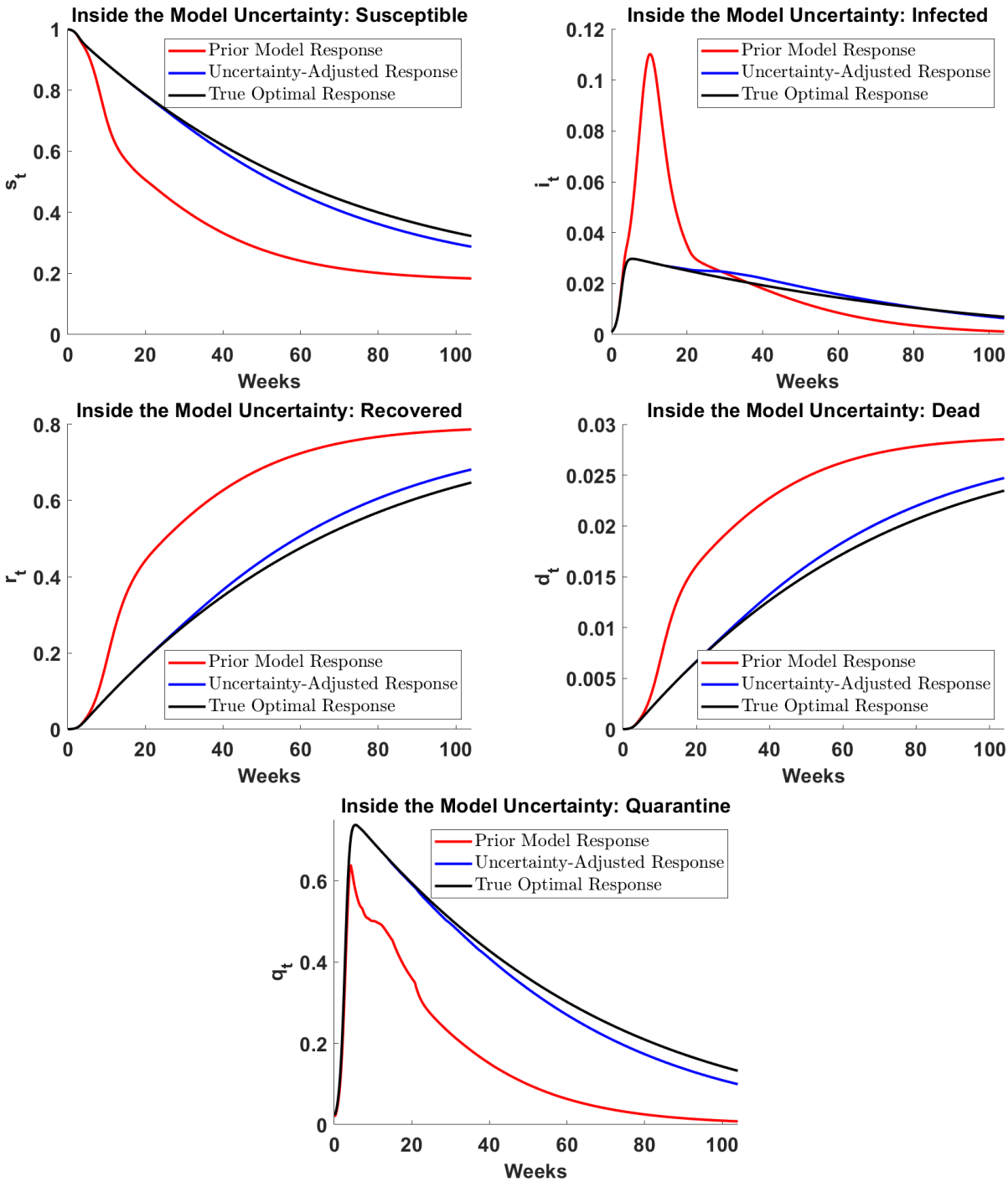

Notes: These figures show (i) the prior model response (red), the true optimal response (black), and the uncertainty-adjusted response (blue) in the case where the policy maker initially underestimates the severity of the pandemic. From left to right, top to bottom, these figures are (1) the fraction of the population that is susceptible to the disease, (2) the fraction of the population that is infected, (3) the fraction of the population that has had the disease and recovered, (4) the fraction of the population that has died, and (5) the fraction of the population in quarantine.

Figure 7: Scenario 1: Underestimating the Pandemic

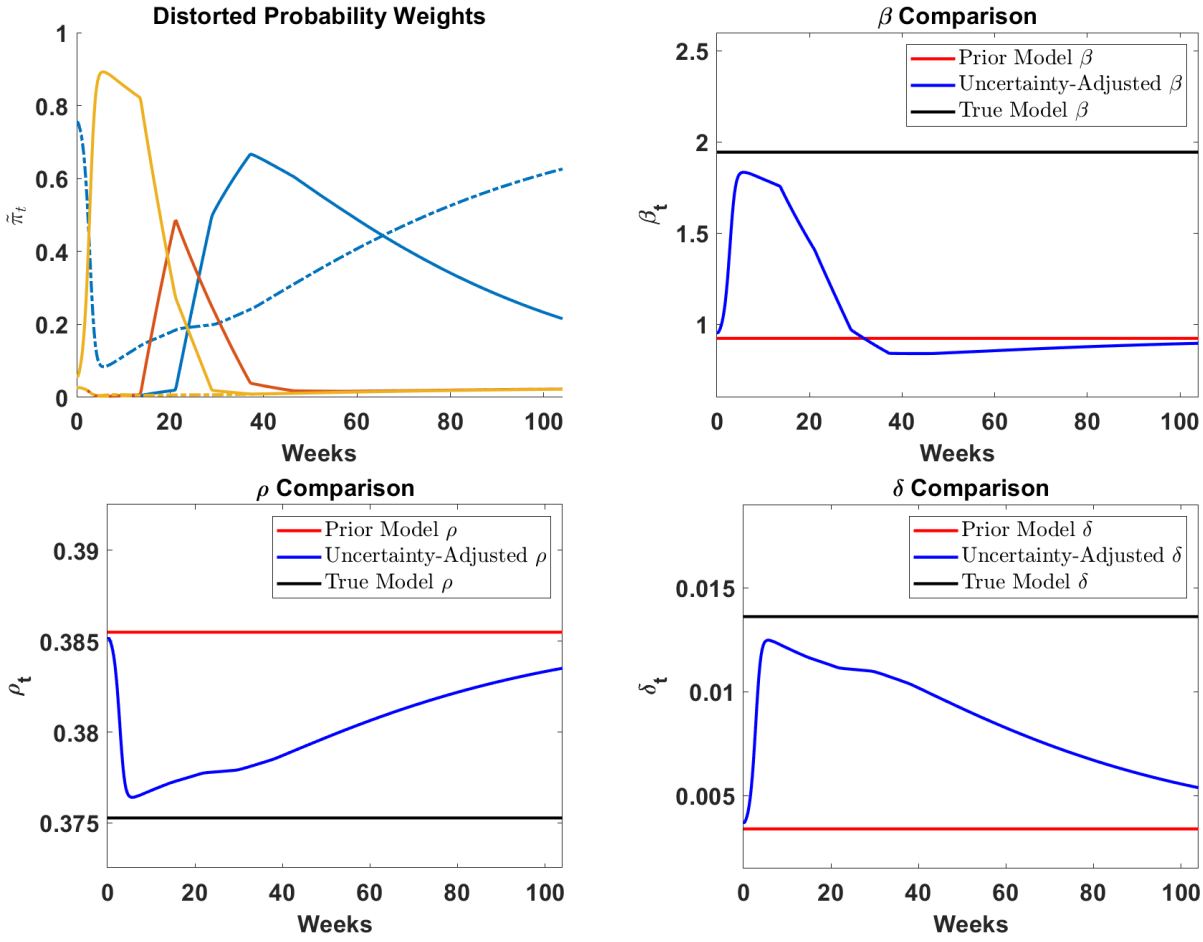

Notes: These figures show (i) the prior model (red), the true model (black), and the uncertainty-adjusted model (blue) parameter value in the case where the policy maker initially underestimates the severity of the pandemic. From left to right, top to bottom, these figures are (1) the distorted probability weights $\tilde{\pi}_t$, (2) the infection rate β_t, (3) the recovery rate ρ_t, and (4) the death rate δ_t. For the distorted probability weights, the blue lines are for models with $\mathcal{R}_0 = 2.0$, the red lines are for models with $\mathcal{R}_0 = 3.5$, the yellow lines are for models with $\mathcal{R}_0 = 5.0$, the dashed-dotted lines are for models with CFR$= 0.005$, the dashed lines are for models with CFR$= 0.020$, and the solid lines are for models with CFR$= 0.035$.

Figure 8: Scenario 2: Correctly Estimating the Pandemic

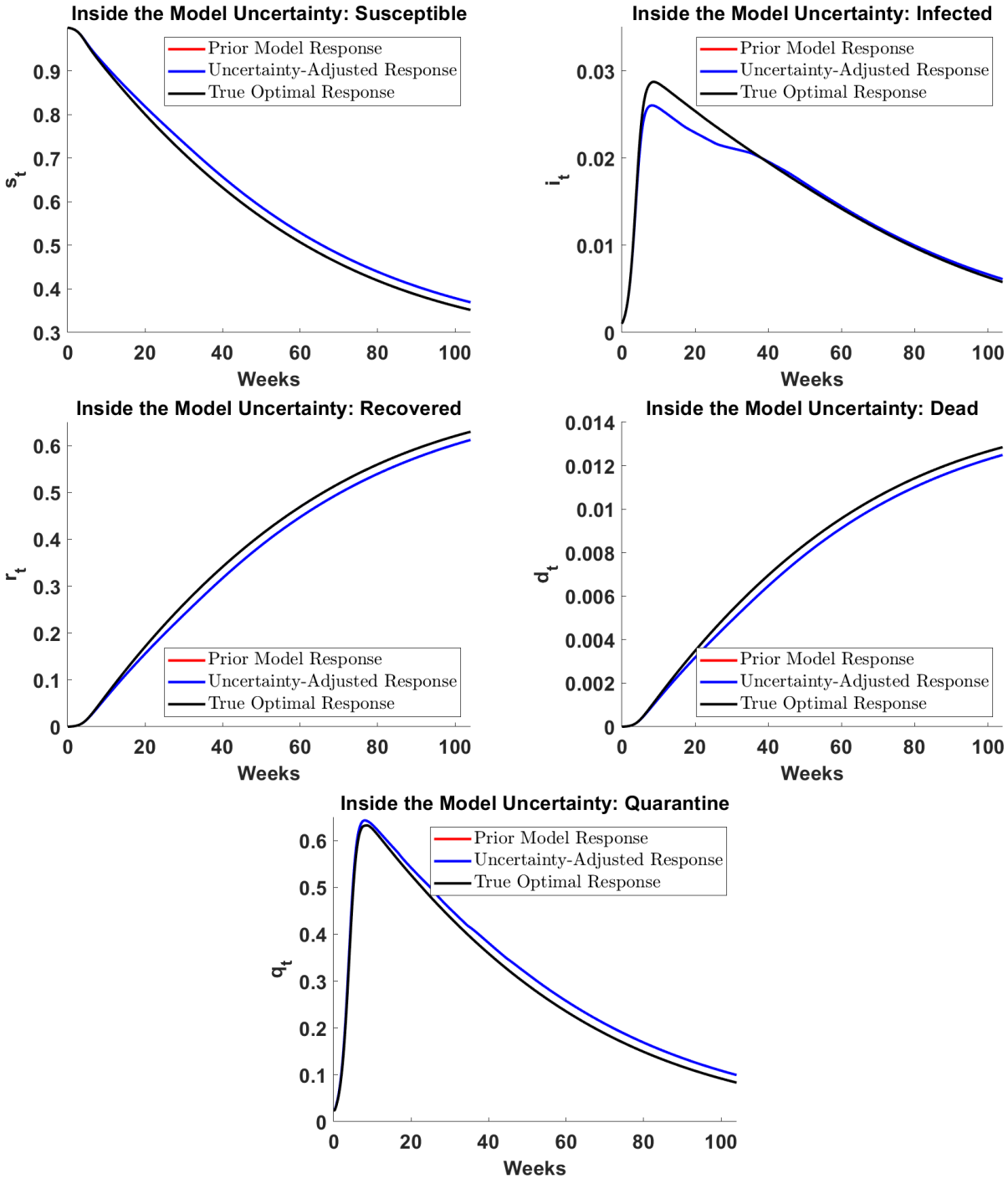

Notes: These figures show (i) the prior model response (red), the true optimal response (black), and the uncertainty-adjusted response (blue) in the case where the policy maker initially correctly estimates the severity of the pandemic. From left to right, top to bottom, these figures are (1) the fraction of the population that is susceptible to the disease, (2) the fraction of the population that is infected, (3) the fraction of the population that has had the disease and recovered, (4) the fraction of the population that has died, and (5) the fraction of the population in quarantine.

Figure 9: Scenario 2: Correctly Estimating the Pandemic

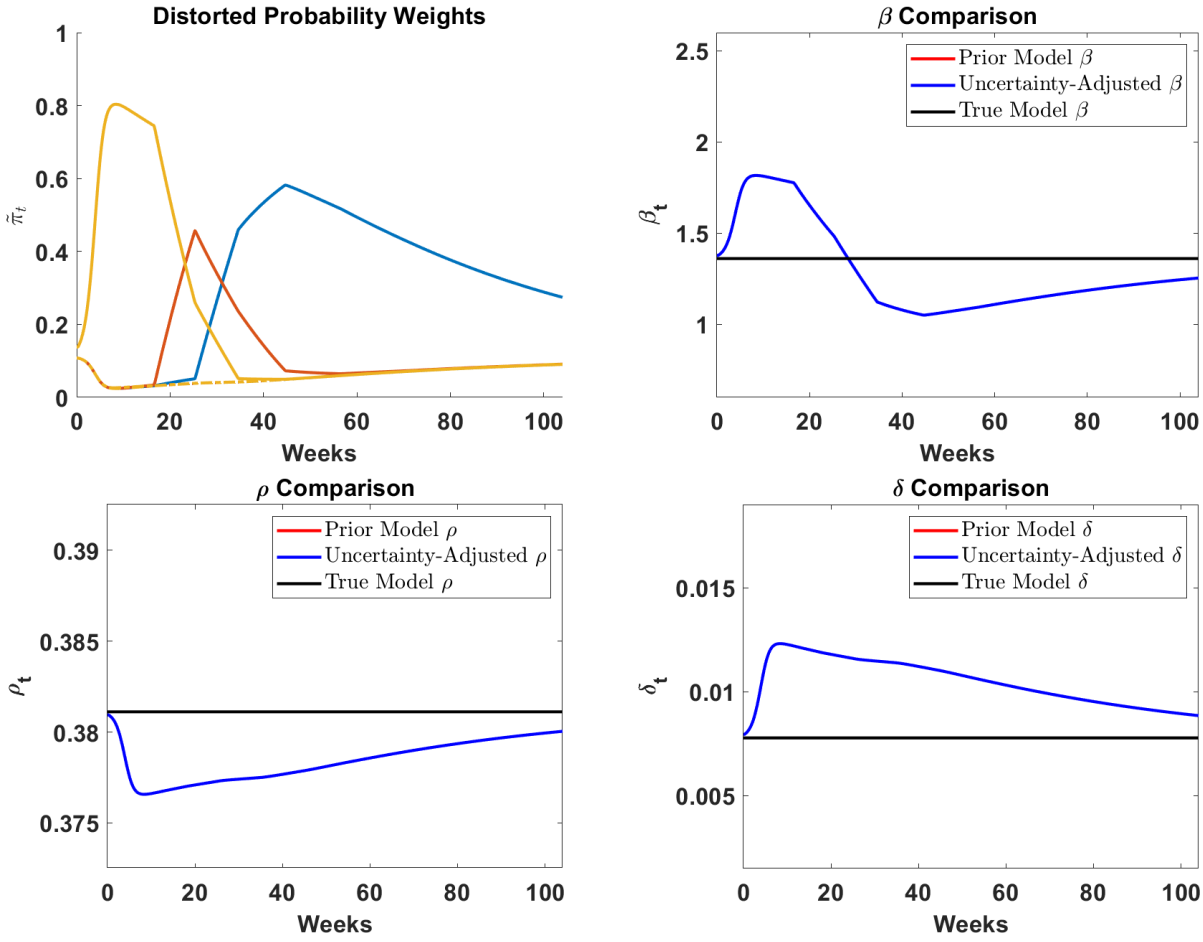

Notes: These figures show (i) the prior model (red), the true model (black), and the uncertainty-adjusted model (blue) parameter value in the case where the policy maker initially correctly estimates the severity of the pandemic. From left to right, top to bottom, these figures are (1) the distorted probability weights $\tilde{\pi}_t$, (2) the infection rate β_t, (3) the recovery rate ρ_t, and (4) the death rate δ_t. For the distorted probability weights, the blue lines are for models with $\mathcal{R}_0 = 2.0$, the red lines are for models with $\mathcal{R}_0 = 3.5$, the yellow lines are for models with $\mathcal{R}_0 = 5.0$, the dashed-dotted lines are for models with CFR$= 0.005$, the dashed lines are for models with CFR$= 0.020$, and the solid lines are for models with CFR$= 0.035$.

Figure 10: Scenario 3: Overestimating the Pandemic

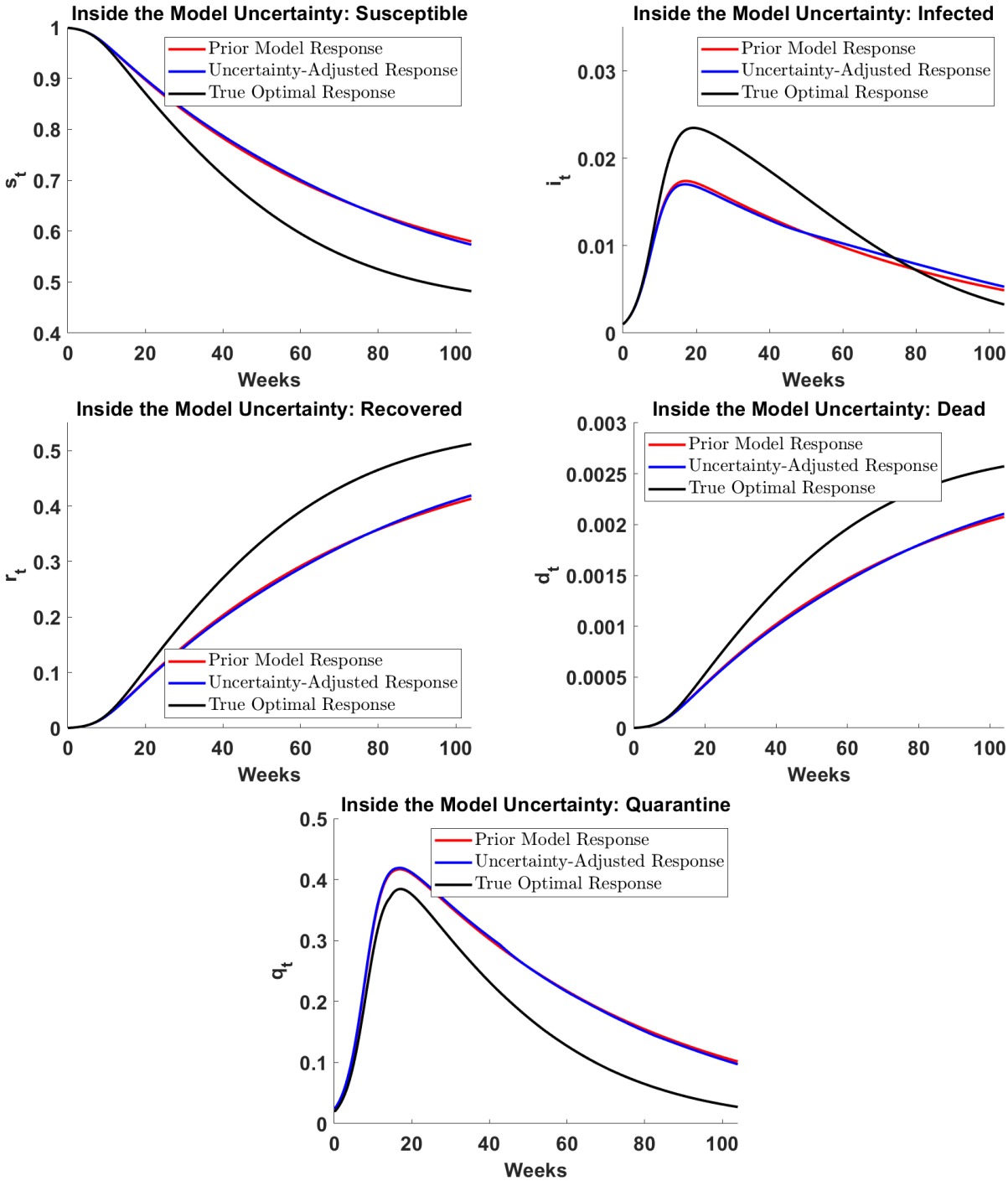

Notes: These figures show (i) the prior model response (red), the true optimal response (black), and the uncertainty-adjusted response (blue) in the case where the policy maker initially overestimates the severity of the pandemic. From left to right, top to bottom, these figures are (1) the fraction of the population that is susceptible to the disease, (2) the fraction of the population that is infected, (3) the fraction of the population that has had the disease and recovered, (4) the fraction of the population that has died, and (5) the fraction of the population in quarantine.

Figure 11: Scenario 3: Overestimating the Pandemic

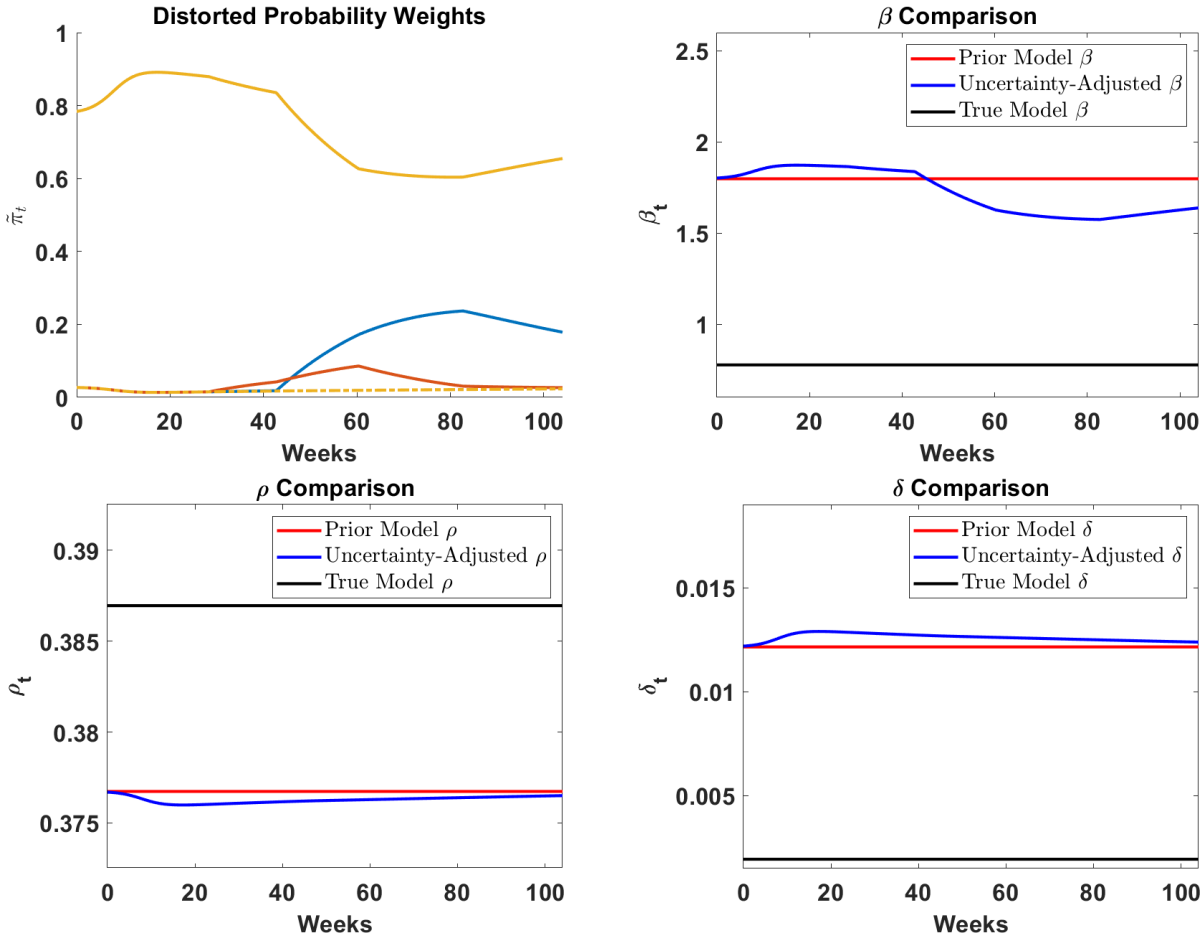

Notes: These figures show (i) the prior model (red), the true model (black), and the uncertainty-adjusted model (blue) parameter value in the case where the policy maker initially overestimates the severity of the pandemic. From left to right, top to bottom, these figures are (1) the distorted probability weights $\tilde{\pi}_t$, (2) the infection rate β_t, (3) the recovery rate ρ_t, and (4) the death rate δ_t. For the distorted probability weights, the blue lines are for models with $\mathcal{R}_0 = 2.0$, the red lines are for models with $\mathcal{R}_0 = 3.5$, the yellow lines are for models with $\mathcal{R}_0 = 5.0$, the dashed-dotted lines are for models with CFR= 0.005, the dashed lines are for models with CFR= 0.020, and the solid lines are for models with CFR= 0.035.

The first case we consider is a case in which models underestimate the severity of the new disease. Here the planner assumes the pandemic has a lower $\mathcal{R}_0$ and CFR than is true. The prior distribution gives the model with $\mathcal{R}_0 = 2$ and CFR$= 0.005$ a weight of 7/9 and the remaining weight equally distributed across the other eight models. The true model parameters are given by $\mathcal{R}_0 = 5$ and CFR$= 0.035$. This case is shown in Figure 6. In this case, the prior model optimal response leads to much lower mitigation efforts relative to the true optimal response. This results in a sharp peak in infections and a much higher death rate relative to the optimal response. The uncertainty adjusted response brings mitigation levels very close to the true optimal, with a corresponding lower infection and death rate.

Figure 7 highlights the underlying mechanisms driving this result. The top left plot shows the distorted probability weights that the planner uses when allowing for uncertainty. Their initial values are driven by the assumed prior, which places a majority of the weight on a low CFR, low $\mathcal{R}_0$ model represented by the dotted-dashed blue line and the remaining weight equally split across all other models. As the pandemic evolves and infections and deaths begin to occur, the planner allowing for uncertainty immediately shifts a significant probability weight to the solid yellow line which represents the model with the highest CFR and $\mathcal{R}_0$ values. This significantly increases the amount of quarantine done and diminishes the impacts of the pandemic. As a result, the pandemic evolves at a much slower rate, leading the planner to shift weight first to the high CFR and middle $\mathcal{R}_0$ value, then to the high CFR and low $\mathcal{R}_0$ value, and finally back towards the model with the highest prior weight. This occurs because the planner is not assumed to be learning, but rather reacting to the observed current state of the pandemic. As a result of this significant uncertainty reaction and strong uncertainty response early on, the pandemic plays out in a way that is nearly as severe as what seemed possible at first, and thus the penalization attached to uncertainty causes the planner to shift their view of what are statistically reasonable worst-case models to consider. A high CFR is persistently relevant for the planner, but because the planner is reacting based on concerns about uncertainty and not learning as in a Bayesian setting, they then begin to revert back to the prior model their decision problem is anchored to.

Intuitively, the penalization costs of allowing for a severe worst-case model are outweighed by the possible gains of making a policy choice that is robust to potentially significant uncertainty. As the pandemic winds down and the effects are limited by the strong early response, the possibility for such large deviations from the assumed prior are less likely and so the planner reduces their uncertainty penalization by considering less severe

worst-case models. The dynamics of the distorted probability weights lead to the remaining outcomes we see in Figure 7. The black and red lines show that the planner initially underestimates the pandemic by assuming a lower β and δ and a higher ρ (the red horizontal lines) than is true (the black horizontal lines). As the pandemic worsens, the uncertain planner shifts their distorted parameters $\tilde{\beta}$, $\tilde{\delta}$ and $\tilde{\rho}$ (the blue lines) away from the prior towards the true values and then winds those values back down towards the prior as the pandemic resolves in a better than first anticipated way.

In the next two cases we consider, incorporating uncertainty has much more muted effects on the optimal response and outcomes. The second case we consider is a case in which models correctly estimate the severity of the new disease. The planner's assumed prior distribution gives each model of $\mathcal{R}_0$ and CFR an equal weight of 1/9 which is the same $\mathcal{R}_0$ and CFR as the true model. This case is shown in Figure 8. In this scenario, incorporating uncertainty into the response has a much more moderate effect. Mitigation efforts, though similar under both the optimal and uncertainty adjusted response, are slightly higher early on and persistently higher over time. Infection and death rates are also similar, though they peak higher under quarantine policy made without consideration for model uncertainty and result in an increase in deaths as well.

Figure 9 demonstrates the underlying mechanisms driving this mode muted response. As in the first scenario, the distorted probability weights start near the assumed prior that gives equal weight to all the models. As before, once the infections and deaths increase the planner then shifts a significant probability weight first to the highest CFR and $\mathcal{R}_0$ model, and the resulting decrease in infections and deaths resulting from the strong quarantine response early on leads to a shift to the high CFR and middle $\mathcal{R}_0$ model and finally to the high CFR and low $\mathcal{R}_0$ model. The probability weights then begin to converge back to the prior, but in this case that means reducing the weight on the high CFR model and increasing weights on all the other models. This response, while similar in the fact that the high CFR models play a key role leading to a strong and fast quarantine response, the differences are far more muted because the pandemic never has a chance to reach the levels of infections and deaths that would lead to drastic uncertainty responses. The planner overreacts by overshooting what the worst case β, ρ, and δ might be at first, but because the true model matches their prior the value of considering more severe worst-case models for longer at the cost of larger uncertainty penalization is never realized.

The third case we consider is a case in which models over estimate the severity of the new disease. The planner here assumes the pandemic has a higher $\mathcal{R}_0$ and CFR than is

true and the assumed prior distribution gives the model with $\mathcal{R}_0 = 5$ and CFR= 0.035 a weight of 7/9 and the remaining weight equally distributed across the remaining eight models. The true model parameters, however, are given by $\mathcal{R}_0 = 2$ and CFR= 0.005. This case is shown in Figure 10. In this case, again incorporating uncertainty into the response has very little effect, and policy and outcomes are nearly identical under the prior model and uncertainty adjusted responses. Both the prior model and the uncertainty adjusted responses lead to overly high mitigation efforts, and low infection and death rates to the optimum given economic damages from the mitigation policy. This result demonstrates the key asymmetry: optimal policy while accounting for uncertainty is significantly closer to the optimal policy when made knowing the true model when underestimating the model, but is no worse than the no uncertainty policy choice in terms of excess quarantine measures and therefore excess economic losses when overestimating the model.

For this scenario, Figure 11 highlights the key model tradeoffs leading to the planner behaving essentially as if he is not uncertain. Because initial distorted probability weights near the assumed prior of a high CFR and high $\mathcal{R}_0$ illicit a higher than optimal quarantine response, the pandemic never reaches states where there is much value to considering more severe worst-case pandemic models at the cost of increased penalization. In fact, there is almost no additional overreaction in this case because infections and deaths increased much slower than the prior model would have suggested. As a result the distorted probability weights stay much more stable and closer to the prior, and only slowly begin to disperse more weight to the models with high CFR and middle and low $\mathcal{R}_0$ values. This causes the planner to maintain a view on the distorted or potential worst case β, ρ, and δ values that also remain very close to the prior values assumed for these parameters. Because of the concern for possible uncertainty, the planner never is able to underreact, which would actually reduce quarantine levels and increase output by allowing more individuals to work. However, uncertainty has essentially no worse economic or welfare implications in this scenario than just assuming the prior model but without aversion to ambiguity.

In future work, we plan to quantify these outcomes in terms of welfare and economic impacts. These valuations will help demonstrate that the effects of model uncertainty, even under relatively modest aversion to uncertainty, can be economically significant and critical to account for in optimal policy decisions related to COVID-19 and other pandemics.

6 Model Extensions

Infection Dependent Death Rate

Following Eichenbaum, Rebelo, and Trabandt (2020) and others, we can account for concerns that the healthcare system could be overwhelmed by the number of infected individuals, leading to an increased CFR. To model this, we can specify, as others have done, that the death rate is given by

$$\delta_t = \delta + \delta_+ i_t^2$$

This framework will not lead to any changes to the functional form for the optimal quarantine choice, but can have significant implications on the value function and will alter the numerical value of the optimal policy choice. Using our framework for understanding uncertainty, we can account for uncertainty about this more generalized specification for the death rate δ_t and determine how this state dependent death rate influences economic outcomes and decisions about quarantine, with and without uncertainty, across the different scenarios that we consider. By taking multiple estimates of δ_+ based on various estimates or measurements from different COVID-19 outbreaks, we can augment our set of pandemic models and conduct a similar analysis to what we have done here to account for this potentially important feature.

Productivity Costs of Mitigation and Uncertainty

An important extension to consider is the possibility of additional costs of quarantine measures on output, beyond the consumption-equivalent costs that result from reduced labor. In addition, a potential consequence of mitigation efforts is that it could lead to reduction in productivity. In particular, Barrot, Grassi, and Sauvagnat (2020) note that social distancing measures could lead to a reduction in GDP growth. We model this formally by extending our expression of productivity to be

$$A = \bar{A}\exp(z_t)$$
$$dz_t = \mu_z dt - \frac{1}{2}\sigma_z^2 dt + \sigma_z dW_t$$

This extends productivity to follow standard geometric Brownian motion growth as is commonly used throughout economics and financial modeling. However, we add to this a

term to account for reduced growth resulting from social distancing quarantine measures, which we will calibrate to fit the estimates provided by Barrot, Grassi, and Sauvagnat (2020). This additional term augments the process for z to now be

$$A = \bar{A}\exp(z_t)$$
$$dz_t = \mu_z dt - \tilde{a}q_t^{\tilde{b}}dt - \frac{1}{2}\sigma_z^2 dt + \sigma_z d\hat{W}_t$$

The cost provides an additional impact from quarantine reflected in not only level impacts but also growth implications for quarantine measures. In addition, as there exists substantial uncertainty about the long-term economic consequences of "shutting down the economy" in this manner, we can allow for this additional channel of model uncertainty as we have done with the pandemic model, allowing for alternative values of $\tilde{a}, \tilde{b}$ to be specified and part of our υ conditional models so that dz_t is given b

$$A = \bar{A}\exp(z_t)$$
$$dz_t = \mu_z dt - \tilde{a}(\upsilon)q_t^{\tilde{b}(\upsilon)}dt - \frac{1}{2}\sigma_z^2 dt + \sigma_z dW_t$$

This additional additional channel of uncertainty will interact with our existing uncertainties and will potentially have meaningful implications for the social planner's optimal policy response to the COVID-19 pandemic.

Uncertainty Through Robustness

Though our analysis mainly used the smooth ambiguity framework, where the social planner optimally chose probability weights to place on competing parameterizations of the model, an alternate approach to the problem is through applying the robust preferences methodology established in the economics literature[14]. Accounting for uncertainty in this way allows the social planner to make optimal mitigation policy choices while acknowledging that a given baseline model may be misspecified. As with smooth ambiguity, the mathematical tractability of the robust preferences decision problem allows us to characterize the implications of uncertainty for optimal policy decisions with clear intuition. We

[14]Detailed explanations of robust preference problems and axiomatic treatment of such formulations using penalization methods are given by Cagetti, Hansen, Sargent, and Williams (2002), Anderson, Hansen, and Sargent (2003), Hansen, Sargent, Turmuhambetova, and Williams (2006), Maccheroni, Marinacci, and Rustichini (2006), and Hansen and Sargent (2011).

briefly outline here how we incorporate robust preferences to account for model uncertainty, and direct readers to the aforementioned references for complete mathematical details.

We define the approximating or baseline model using the evolution equations of the state variables as previously given:

$$\begin{aligned} ds_t &= -\beta(s_t - q_t)i_t dt - \sigma_\beta i_t dW_t \\ di_t &= \beta(s_t - q_t)i_t dt - (\rho + \delta)i_t dt + \sigma_\beta i_t dW_t - \sigma_\delta i_t dW_t \\ dd_t &= \delta i_t dt + \sigma_\delta i_t dW_t \end{aligned}$$

As was the case in the smooth ambiguity setting, we assume the baseline model is the result of historical data or previous information about coronavirus pandemics and acts as a best-guess at what the true COVID-19 pandemic model is for policymakers. However, we allow the social planner in our model to consider the likelihood that this model is misspecified, or that there are possibly other models which are the true model for the COVID-19 pandemic.

Possible alternative models are represented by a drift distortion that is added to the approximating model by changing the Brownian motion W_t to $\hat{W}_t + \int_0^t h_s ds$ where h_s and $\hat{W}_t$ are processes adapted to the filtration generated by the Brownian motion W_t. Therefore, alternative models under consideration by the social planner are of the form

$$\begin{aligned} ds_t &= [-\beta(s_t - q_t)i_t - h_t\sigma_\beta i_t]dt - \sigma_\beta i_t d\hat{W}_t \\ di_t &= [\beta(s_t - q_t)i_t - (\rho + \delta)i_t + h_t\sigma_\beta i_t - h_t\sigma_\delta i_t]dt + \sigma_\beta i_t d\hat{W}_t - \sigma_\delta i_t d\hat{W}_t \\ dd_t &= [\delta i_t + h_t\sigma_\delta i_t]dt + \sigma_\delta i_t d\hat{W}_t \end{aligned}$$

In this form, the alternative models are disguised by the Brownian motion and so are hard to detect statistically using past data. In addition, the alternative models are given without direct parametric form, which allows for a larger class of alternative models under consideration by the planner.

We can interpret the drift perturbations for misspecification directly as parameter misspecifications and altered model parameters of the form

$$\begin{aligned} ds_t &= [-\tilde{\beta}(s_t - q_t)i_t]dt - \sigma_\beta(s_t - q_t)i_t dW_t \\ di_t &= [\tilde{\beta}(s_t - q_t)i_t - (\rho + \tilde{\delta})i_t]dt + \sigma_\beta(s_t - q_t)i_t dW_t - \sigma_\delta i_t dW_t \\ dd_t &= [\tilde{\delta} i_t]dt + \sigma_\delta i_t dW_t \end{aligned}$$

where $\tilde{\beta} = \beta + \frac{h_t \sigma_\beta}{(s-q)}$ and $\tilde{\delta} = \delta + h_t \sigma_\delta$. The h_t in the model will be optimally determined and state dependent, and so the magnitude of the parameter misspecification considered by the social planner when making optimal policy decisions will depend on the current state of the pandemic and evolve dynamically.

For the uncertainty analysis to be reasonable, we will restrict the set of alternative models considered by the social planner to those that are difficult to distinguish from the baseline model using statistical methods and past data. A penalization term based on the conditional relative entropy measure of model distance is used to accomplish this. The parameter θ_m is chosen to determine the magnitude of this penalization. We have defined relative entropy previously, and note that Hansen, Sargent, Turmuhambetova, and Williams (2006) provides complete details about relative entropy use in a robust preferences setting. Again, relative entropy means we are only considering relatively small, though potentially significant, distortions from the baseline model.

The time derivative of relative entropy or contribution of the current worst-case model $h_t dt$ to relative entropy is given by $\frac{1}{2}|h_t|^2$. This term is added to the flow utility or preferences of the household to account for model uncertainty. As was the case in the smooth ambiguity setting, optimal decisions will be determined by considering alternative worst-case models as a device to generate optimal policies that are robust to alternative models, and not as some type of distorted beliefs setting. The household maximization problem is replaced with a max-min set-up, where the minimization is made over possible model distortions h_t^* which are constrained by θ_m. This allows the planner to determine the relevant worst-case model for given states of the world to help inform their optimal policy decisions.

While we have incorporated additional structure and complexity to the model to account for model uncertainty, the resulting household or social planner problem remains tractable and similar to the previous, no uncertainty problem, and is given by

$$V(s_t, i_t, d_t) = \max_{q_t} \min_{h_t} E_0[\int_0^\infty \{\log(C_t) + \frac{\theta}{2}|h_t|^2\} dt]$$

subject to market clearing and labor supply constraints.

As before, the social planner's solution is still characterized by a recursive Markov equilibrium for which an equilibrium solution is defined as before. The HJB equation resulting from this modified household or social planner optimization problem which characterizes

the socially optimal solution is now given by

$$\begin{aligned}0 = -\kappa V + \kappa \log[AL(1 - i_t - d_t - q_t)] + \frac{\theta}{2}|h_t|^2 \\ +V_s[-\beta(s_t - q_t)i_t - h_t\sigma_\beta i_t] + V_i[\beta(s_t - q_t)i_t - (\rho + \delta)i_t + h_t\sigma_\beta i_t - h_t\sigma_\delta i_t] \\ +V_d[\delta i_t + h_t\sigma_\delta i_t] + \frac{1}{2}\{V_{ss}\sigma_\beta^2 + V_{ii}[\sigma_\beta^2 + \sigma_\delta^2] + V_{dd}\sigma_\delta^2\}i_t^2 \\ -\{\sigma_\beta^2 V_{si} + \sigma_\delta^2 V_{id}\}i_t^2\end{aligned}$$

The first-order conditions for the optimal model distortions give us

$$|h_t|^2 = \frac{1}{\theta^2}[(V_i - V_s)^2(\sigma_\beta i_t)^2 + (V_d - V_i)^2(\sigma_\delta i_t)^2]$$

Plugging back in to the HJB equation, we are left with the following problem

$$\begin{aligned}0 = -\kappa V + \kappa \log[AL(1 - i_t - d_t - q_t)] \\ -\frac{1}{2\theta}[(V_i - V_s)^2(\sigma_\beta i_t)^2 + (V_d - V_i)^2(\sigma_\delta i_t)^2] \\ +V_s[-\beta(s_t - q_t)i_t] + V_i[\beta(s_t - q_t)i_t - (\rho + \delta)i_t] + V_d[\delta i_t] \\ +\frac{1}{2}\{V_{ss}\sigma_\beta^2 + V_{ii}[\sigma_\beta^2 + \sigma_\delta^2] + V_{dd}\sigma_\delta^2\}i_t^2 \\ -\{\sigma_\beta^2 V_{si} + \sigma_\delta^2 V_{id}\}i_t^2\end{aligned}$$

The optimal choice of mitigation q_t is the solution to a quadratic equation resulting from the first-order condition and is given by

$$q_t = \frac{-(\kappa ALa) \pm \sqrt{(\kappa ALa)^2 + ALa(V_s - V_i)^2(\beta i_t)^2[AL(1 - i - d) - \gamma_1 i - \gamma_2 \rho i]}}{ALa(V_s - V_i)(\beta i_t)}$$

Key differences to the social planner problem and HJB equation show up through the adjustments to the flow utility as a result of the penalization term accounting for model uncertainty concerns. The optimal mitigation policy takes the same functional form as before. The implications of model uncertainty for optimal mitigation policy and social welfare in the face of a pandemic are not only the direct adjustments to the key equations of interest, but also how these adjustments feed through the model solution and alter the value function V and the marginal values of changes to the susceptible, infected, and dead populations, represented by V_s, V_i, V_d. Though we do not report results from this approach, the high-level findings mirror closely those under the smooth ambiguity approach.

6.1 Disciplining our analysis of model uncertainty

As we have introduced new parameters to our model, the parameters for model uncertainty θ_a and θ_m, it is important to discipline them in a meaningful way. To do this for the robustness case, we can calibrate θ_m based on bounds of statistical model discrimination based on methods developed and extended by Chernoff (1952), Newman and Stuck (1979), and Anderson, Hansen, and Sargent (2003). Furthermore, the spread on estimates from the recent papers estimating the CFR and $\mathcal{R}_0$ will provide further anecdotal constraints. Solving the model and determining the magnitude of relative entropy and model distortion implied by the choice of θ_m, we can compare how these distortions compare to the parameter values estimated in the literature and the implied statistical discrimination bounds to determine reasonable values of θ_m. We can then compare these bounds and results to the smooth ambiguity case to determine reasonable values of θ_a as well. While we currently use values of θ_m and θ_m that impose significant amounts of uncertainty aversion without calibrating them, we plan to use these methods going forward.

The method of statistical model discrimination we will use is for the robustness based uncertainty measure is based on bounds derived by Chernoff (1952) for the error of statistical detection between two models and Newman and Stuck (1979) who derived this bound for a Markov counterpart. The bounds are based on a simplified, two-case model detection problem where a decision maker tries statistically discriminate between the baseline model and the worst-case model. The relevant bound comes from determining the probability that the decision maker makes a type I or type II error in determining the true model while choosing between the two possible models. We focus on an approximation of this bound demonstrated by Anderson, Hansen, and Sargent (2000), Anderson, Hansen, and Sargent (2003), and Hansen, Sargent, Turmuhambetova, and Williams (2006) that uses a minimization of the implied local decay rate bound

$$\varepsilon_N \leqslant = \frac{1}{2} exp(-N\Theta')$$

where Θ' is given by

$$\Theta' = \max_{0 \leqslant r \leqslant 1} \frac{1}{2}(r-1) r h_t h_t' = \frac{1}{8} h_t h_t'.$$

Here ε_N is the probability of making a type I or type II error in detecting the true model and N is the data sample size. We use $N = 260$ weeks, or 5 years for our sample size to

learn from. This approximate bound is still a conditional measure of model discrimination that is state-dependent, and we will use this to discipline what is a reasonable value of θ, along with comparisons of the distorted model parameters to estimates from other papers studying COVID-19, for our analysis of model misspecification.

7 Concluding Remarks

This paper shows how to incorporate uncertainty in models of pandemics. Our main results focus on the role of uncertainty aversion in a smooth ambiguity-based decision problem, but we also show how a robust control approach would be implemented as well. With new diseases, or diseases that have only had small outbreaks, there is often significant uncertainty about key parameters which determine the overall costs of an epidemic. The results highlight important asymmetries that may be present in many robust control problems. Incorporating uncertainty into responses are particularly important when the assumed prior model underestimates the severity of a new threat in terms of responding in a way that is much closer to the optimal response when the true model is know. On the other hand, though incorporating uncertainty does lead to an overreaction compared to traditional approaches when the assumed prior matches the true model, the overreaction is fairly moderate and the uncertainty-based response and traditional approach are nearly identical when the assumed prior model overestimates the true values of a new threat.

Our analysis provides a framework under which uncertainty and model misspecification can be incorporated into macroeconomic models of epidemics. Our work emphasizes the that uncertainty can play a large role in determining the optimal policy response to a new disease. Economists and epidemiologists, rather than using a range of parameters, can use our framework to explicitly model uncertainty. Future work can focus on making these models more tractable for policymakers, who often have to make decisions in real time.

References

Acemoglu, D., V. Chernozhukov, I. Werning, and M. Whinston (2020). A multi-risk sir model with optimally targeted lockdown. Technical report, National Bureau of Economic Research.

Allcott, H., L. Boxell, J. Conway, M. Gentzkow, M. Thaler, and D. Y. Yang (2020). Polarization and public health: Partisan differences in social distancing during the coronavirus pandemic. *NBER Working Paper* (w26946).

Anderson, E., L. P. Hansen, and T. J. Sargent (2000). Robustness, Detection and the Price of Risk. *Working Paper*.

Anderson, E. W., L. P. Hansen, and T. J. Sargent (2003). A Quartet of Semigroups for Model Specification, Robustness, Prices of Risk, and Model Detection. *Journal of the European Economic Association 1*(1), 68–123.

Arrow, K. J. (1951). Alternative approaches to the theory of choice in risk-taking situations. *Econometrica: Journal of the Econometric Society*, 404–437.

Atkeson, A. (2020a). How deadly is covid-19? understanding the difficulties with estimation of its fatality rate. Technical report, National Bureau of Economic Research.

Atkeson, A. (2020b). What will be the economic impact of covid-19 in the us? rough estimates of disease scenarios. Technical report, National Bureau of Economic Research.

Avery, C., W. Bossert, A. Clark, G. Ellison, and S. F. Ellison (2020). Policy implications of models of the spread of coronavirus: Perspectives and opportunities for economists. Technical report, National Bureau of Economic Research.

Baker, S. R., N. Bloom, and S. J. Davis (2016). Measuring economic policy uncertainty. *The Quarterly Journal of Economics 131*(4), 1593–1636.

Baker, S. R., N. Bloom, S. J. Davis, and S. J. Terry (2020). Covid-induced economic uncertainty. Technical report, National Bureau of Economic Research.

Baker, S. R., R. A. Farrokhnia, S. Meyer, M. Pagel, and C. Yannelis (2020a). How does household spending respond to an epidemic? consumption during the 2020 covid-19 pandemic. Technical report, National Bureau of Economic Research.

Baker, S. R., R. A. Farrokhnia, S. Meyer, M. Pagel, and C. Yannelis (2020b). Income, liquidity, and the consumption response to the 2020 economic stimulus payments. Technical report, National Bureau of Economic Research.

Baldauf, M., L. Garlappi, and C. Yannelis (2019). Does climate change affect real estate prices? only if you believe in it. *Review of Financial Studies, Forthcoming*.

Barnett, M., W. Brock, and L. P. Hansen (2019). Pricing Uncertainty Induced by Climate Change. *University of Chicago Becker Friedman Institute for Economics Working Paper No. 2019-109. Available at SSRN: https://ssrn.com/abstract=3440301*.

Barnett, M., W. Brock, and L. P. Hansen (2020). Pricing uncertainty induced by climate change. *The Review of Financial Studies 33*(3), 1024–1066.

Barrios, J. and Y. Hochberg (2020). Risk perception through the lens of politics in the time of the covid-19 pandemic. *Working Paper*.

Barro, R. J., J. F. Ursúa, and J. Weng (2020). The coronavirus and the great influenza pandemic: Lessons from the "spanish flu" for the coronavirus's potential effects on mortality and economic activity. Technical report, National Bureau of Economic Research.

Barrot, J.-N., B. Grassi, and J. Sauvagnat (2020). Sectoral effects of social distancing. *Working Paper*.

Bloom, N. (2009). The impact of uncertainty shocks. *Econometrica 77*(3), 623–685.

Burke, M., W. M. Davis, and N. S. Diffenbaugh (2018). Large Potential Reduction in Economic Damages Under UN Mitigation Targets. *Nature 557*(7706), 549.

Cagetti, M., L. P. Hansen, T. Sargent, and N. Williams (2002). Robustness and pricing with uncertain growth. *The Review of Financial Studies 15*(2), 363–404.

Chater, N. (2020). Facing up to the uncertainties of covid-19. *Nature Human Behaviour*, 1–1.

Chen, Z. and L. Epstein (2002). Ambiguity, risk, and asset returns in continuous time. *Econometrica 70*(4), 1403–1443.

Chernoff, H. (1952). A measure of asymptotic efficiency for tests of a hypothesis based on the sum of observations. *The Annals of Mathematical Statistics*, 493–507.

Coibion, O., Y. Gorodnichenko, and M. Weber (2020). Labor markets during the covid-19 crisis: A preliminary view. *Fama-Miller Working Paper*.

Colacito, R., B. Hoffmann, and T. Phan (2018). Temperatures and growth: A panel analysis of the united states. *Journal of Money, Credit, and Banking 51*(2-3), 2019.

Coven, J. and A. Gupta (2020). Disparities in mobility responses to covid-19. Technical report.

Dell, M., B. F. Jones, and B. A. Olken (2012). Temperature Shocks and Economic Growth: Evidence from the Last Half Century. *American Economic Journal: Macroeconomics 4*(3), 66–95.

Eichenbaum, M. S., S. Rebelo, and M. Trabandt (2020). The macroeconomics of epidemics. Technical report, National Bureau of Economic Research.

Gilboa, I., D. Schmeidler, et al. (1989). Maxmin expected utility with non-unique prior. *Journal of Mathematical Economics 18*(2), 141–153.

Gormsen, N. J. and R. S. Koijen (2020). Coronavirus: Impact on stock prices and growth expectations. *University of Chicago, Becker Friedman Institute for Economics Working Paper* (2020-22).

Granja, J., C. Makridis, C. Yannelis, and E. Zwick (2020). Did the paycheck protection program hit the target? *National Bureau of Economic Research Working Paper*.

Hambel, C., H. Kraft, and E. Schwartz (2015, March). Optimal Carbon Abatement in a Stochastic Equilibrium Model with Climate Change. Working Paper 21044, National Bureau of Economic Research.

Hansen, L. and T. J. Sargent (2001). Robust control and model uncertainty. *American Economic Review 91*(2), 60–66.

Hansen, L. P. and J. Miao (2018). Aversion to ambiguity and model misspecification in dynamic stochastic environments. *Proceedings of the National Academy of Sciences 115*(37), 9163–9168.

Hansen, L. P. and T. J. Sargent (2007). Recursive robust estimation and control without commitment. *Journal of Economic Theory 136*(1), 1–27.

Hansen, L. P. and T. J. Sargent (2011). Robustness and Ambiguity in Continuous Time. *Journal of Economic Theory 146*(3), 1195–1223.

Hansen, L. P. and T. J. Sargent (2019). Structured uncertainty and model misspecification. *University of Chicago, Becker Friedman Institute for Economics Working Paper* (2018-77).

Hansen, L. P., T. J. Sargent, G. Turmuhambetova, and N. Williams (2001). Robustness and uncertainty aversion. *Manuscript, University of Chicago*.

Hansen, L. P., T. J. Sargent, G. Turmuhambetova, and N. Williams (2006). Robust Control and Model Misspecification. *Journal of Economic Theory 128*(1), 45–90.

Hsiang, S., R. Kopp, A. Jina, J. Rising, M. Delgado, S. Mohan, D. Rasmussen, R. Muir-Wood, P. Wilson, M. Oppenheimer, et al. (2017). Estimating Economic Damage from Climate Change in the United States. *Science 356*(6345), 1362–1369.

Jones, C., T. Philippon, and V. Venkateswaran (2020). Optimal mitigation policies in a pandemic. *Working Paper*.

Kaplan, G., B. Moll, and G. Violante (2020). Pandemics according to hank. Technical report, Working Paper.

Klibanoff, P., M. Marinacci, and S. Mukerji (2005). A Smooth Model of Decision Making Under Ambiguity. *Econometrica 73*(6), 1849–1892.

Knight, F. H. (1971). Risk, uncertainty and profit, 1921. *Library of Economics and Liberty*.

Korolev, I. (2020). Identification and Estimation of the SEIRD Epidemic Model for COVID-19. *Working Paper*.

Maccheroni, F., M. Marinacci, and A. Rustichini (2006). Ambiguity Aversion, Robustness, and the Variational Representation of Preferences. *Econometrica*, 1447–1498.

Manski, C. F. and F. Molinari (2020). Estimating the covid-19 infection rate: Anatomy of an inference problem. Technical report, National Bureau of Economic Research.

Newman, C. M. and B. Stuck (1979). Chernoff bounds for discriminating between two markov processes. *Stochastics: An International Journal of Probability and Stochastic Processes 2*(1-4), 139–153.

Spychalski, P., A. Błażyńska-Spychalska, and J. Kobiela (2020). Estimating case fatality rates of covid-19. *The Lancet Infectious Diseases*.

Stock, J. H. (2020). Data gaps and the policy response to the novel coronavirus. Technical report, National Bureau of Economic Research.

Wang, H., Z. Wang, Y. Dong, R. Chang, C. Xu, X. Yu, S. Zhang, L. Tsamlag, M. Shang, J. Huang, et al. (2020). Phase-adjusted estimation of the number of coronavirus disease 2019 cases in wuhan, china. *Cell discovery 6*(1), 1–8.

Appendix A Parameter Values

This appendix discusses the parameter values used in the main calibration. These parameters are shown the table below.

Table A.1: Parameter Values

Parameters	Variable	Value
Non-Pandemic Output	$A \times L$	0.3846
Case Fatality Rate	CFR	$\{0.005, 0.02, 0.035\}$
Reproduction Number	$\mathcal{R}_0$	$\{2.0, 3.5, 5.0\}$
Infection Half Life	γ	$\frac{7}{18}$
Infection Rate	β	$\mathcal{R}_0 \times \gamma$
Death Rate	δ	CFR$\times\gamma$
Recovery Rate	ρ	$(1 - CFR) \times \gamma$
Subjective Discount Rate	κ	0.0003846
Mitigation Costs	$\{a, b\}$	$\{1.25, 2\}$
Volatilies	$\sigma_\beta, \sigma_\delta$	$\{0.1, 0.05\}$
Ambiguity Parameter	θ_a	$\{0.00004, 1000\}$
Robustness Parameter	θ_m	$\{0.0067, 1000\}$

Appendix B Numerical Solution Method

The numerical method we implement here has been used and developed in other papers, including Barnett et al. (2019), and the summary of this algorithm that we provide here closely follows what has been outlined in those papers[15]. We solve the HJB equations that are given by nonlinear partial differential equations using the method of false transient with an implicit finite difference scheme and conjugate gradient solver. The PDEs can be expressed in a conditionally linear form given by

$$\begin{aligned} 0 &= V_t(x) + A(x; V, V_x, V_{xx})V(x) + B(x; V, V_x, V_{xx})V_x(x) \\ &\quad + \frac{1}{2} tr[C(x; V, V_x, V_{xx})V_{xx}(x)C(x; V, V_x, V_{xx})] + D(x; V, V_x, V_{xx}) \end{aligned}$$

x is a state variable vector and $V_x(x) = \frac{\partial V}{\partial x}(x), V_{xx}(x) = \frac{\partial^2 V}{\partial x \partial x'}(x)$ are used for notational simplicity. The agent has an infinite horizon and so the problem is time stationary. Thus, $V_t(x) = \frac{\partial V}{\partial t}(x)$ has been added as a "false transient" in order to construct the iterative solution algorithm. In particular, the solution comes by finding a $V(x)$ such that the above equality holds and $V_t(x) = 0$.

The solution is found by first guessing a value function $V^0(x)$. Approximate derivatives $\widetilde{V_x^0}(x)$ and $\widetilde{V_{xx}^0}(x)$ are calculated from $V^0(x)$ using central finite differences (except at the boundaries where central differences require points outside the discretized state space and so appropriate forward or backward differences are used). These derivatives are used to calculate the coefficients A, B, C and D, and depend on the value function and its derivatives because of the maximization from choosing optimal controls $\{i_k, i_R, N\}$ in order to maximize utility. Applying a backward difference for $V_t^0(x)$, plugging in the calculated coefficients to the conditionally linear system, and rearranging gives

$$\begin{aligned} V^1(x) &= V^0(x) + [A(x, V^0, \widetilde{V_x^0}, \widetilde{V_{xx}^0})V^0(x) + B(x, V^0, \widetilde{V_x^0}, \widetilde{V_{xx}^0})\widetilde{V_x^0}(x) \\ &\quad + \frac{1}{2} tr[C(x, V^0, \widetilde{V_x^0}, \widetilde{V_{xx}^0})\widetilde{V_{xx}^0}(x)C(x, V^0, \widetilde{V_x^0}, \widetilde{V_{xx}^0})] + D(x, V^0, \widetilde{V_x^0}, \widetilde{V_{xx}^0})]\Delta t \end{aligned}$$

We then solve numerically for $V^1(x)$ and repeat this process, with the solution at each iteration k serving as the guess for the next iteration $k+1$, until $\max_x \frac{|V^{k+1}(x) - V^k(x)|}{\Delta t} < tol$ for a specified $tol > 0$. The choice of Δt is made by trading off increases in speed of convergence, achieved by increasing the size of Δt, and maintaining stability of the iterative

[15] Joseph Huang, Paymon Khorrami, Fabrice Tourre, and the research professionals at the Macro Finance Research Program helped in developing the software for this solution method.

algorithm, achieved by decreasing Δt.

The equation for $V^1(x)$ can be expressed as a linear system $\Lambda\chi = \pi$, whose solution at each iteration is found by using the conjugate gradient method. This method uses an iterative method to minimize the quadratic expression $\frac{1}{2}\chi'\Lambda\chi - \chi'\pi$. The χ that minimizes this expression is equivalent to the solution of the linear system if Λ is positive definite as the first-order condition for the minimization problem requires $\Lambda\chi - \pi = 0$. While my Λ is not necessarily symmetric, because it is invertible we can transform our system to $\Lambda'\Lambda\chi = \Lambda'\pi \iff \hat{\Lambda}\chi = \hat{\pi}$ which satisfies the necessary conditions and has the same solution as our original linear system.

Table A.2 provides values used for the state space discretization and hyper-parameters needed for the numerical algorithm used to solve my model. Δt refers to the false transient step size referred to above, ϵ is the tolerance set for the false transient convergence algorithm, ns, ni, nd are the discretization step sizes for the states variables, and $s_{max}, i_{max}, d_{max}, s_{min}, i_{min}, d_{min}$ are the maximum and minimum values for the discretized state space.

An important numerical issue to consider in this framework is that the state space has an important adding up constraint that $1 = s_t + i_t + r_t + d_t$. We have limited the discretized state space to focus on the relevant regions of each population to achieve an accurate approximation, but we also limit the number of points where this adding up constraint is violated. While various boundary condition methods can be used in cases where points violate the adding up constraint, such as Dirichlet or reflective boundary conditions, we use an interpolative Neumann boundary to approximate the derivative of the value function at these points based on nearest points that satisfy the adding up constraint. We tried various state regions to try to verify that our numerical framework provides consistent and robust solutions.

Appendix C Uncertainty Through Robustness Results

This section provides additional robustness results, corresponding to the model presented in section 6. We apply a slightly simplified version of the three scenario exercise done with the smooth ambiguity model.

The first case we consider is a case in which models underestimate the severity of the new disease. Here the planner assumes the pandemic has a lower $\mathcal{R}_0$ and CFR than is true. The baseline model assumes $\mathcal{R}_0 = 2$ and CFR$= 0.005$, while the true model is $\mathcal{R}_0 = 5$ and

Table A.2: Numerical hyper-parameters

FT step size	Δt	0.05
Tolerance parameter	ϵ	$1e-12$
s step size	ns	0.0750
i step size	ni	0.0333
d step size	nd	0.0037
s max value	s_{max}	1.0
i max value	i_{max}	0.4
d max value	d_{max}	0.03
s min value	s_{min}	0.0
i min value	i_{min}	0.0
i min value	d_{min}	0.0

CFR= 0.035. This case is shown in Figure A.1. The results and intuition are very similar to those shown in Figure 6 and discussed thereafter.

The second case we consider is a case in which models correctly estimate the severity of the new disease. The planner's assumed baseline model assumes $\mathcal{R}_0 = 3.5$ and CFR= 0.02, which matches the true model. This case is shown in Figure A.2. Again, the results and intuition are nearly identical to those shown in Figure 8 and discussed thereafter.

The third case we consider is a case in which models over estimate the severity of the new disease. The planner here assumes the baseline pandemic model of $\mathcal{R}_0 = 5.0$ and CFR= 0.035, while the true pandemic model is $\mathcal{R}_0 = 2.0$ and CFR= 0.005. This case is shown in Figure A.3. As with the previous two cases, the results and intuition are essentially identical to those shown in Figure 10 and discussed thereafter.

Figure A.1: Scenario 1: Underestimating the Pandemic

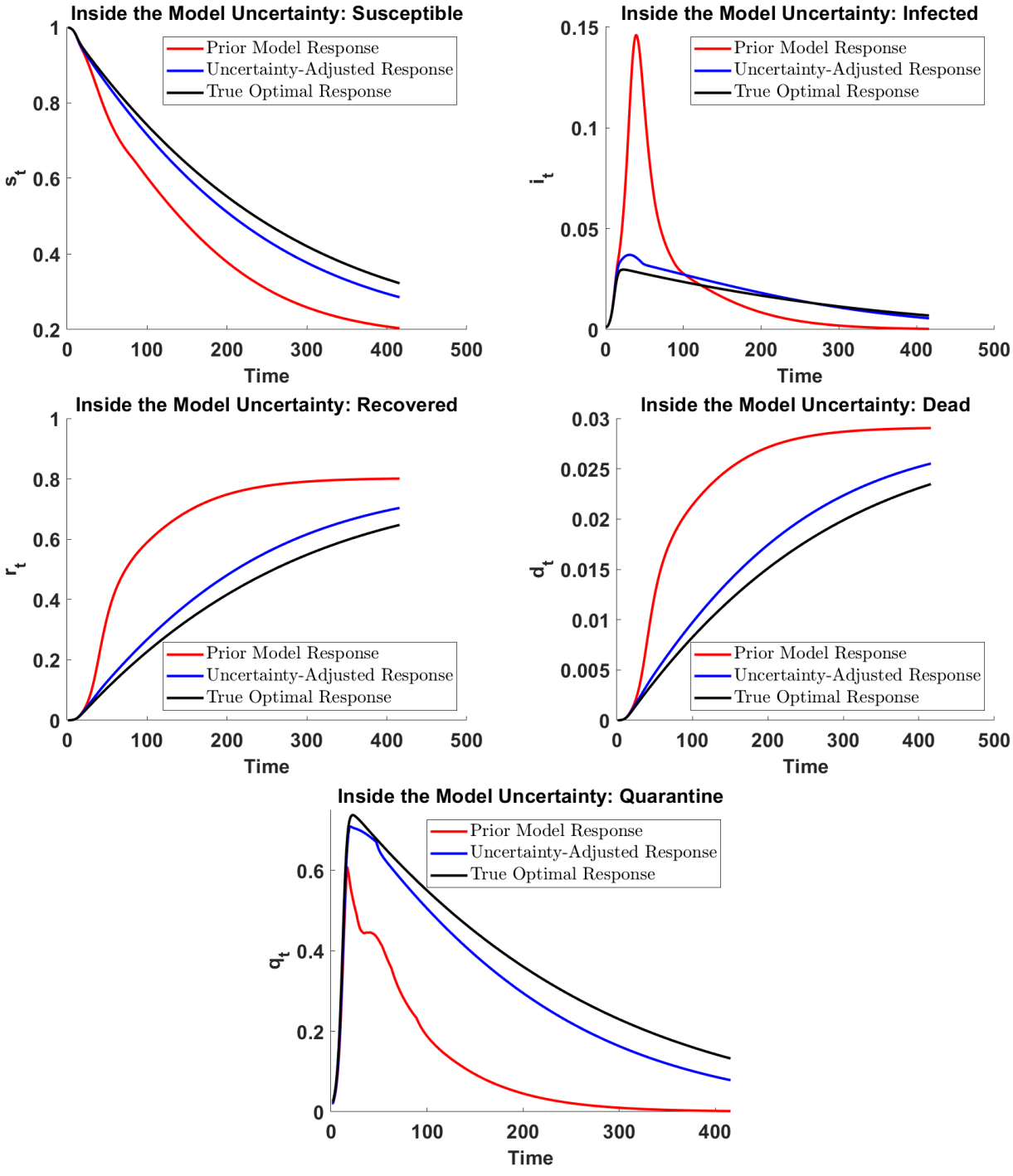

Notes: These figures show (i) the prior model response (red), the true optimal response (black), and the uncertainty-adjusted response (blue) in the case where the policy maker initially underestimates the severity of the pandemic. From left to right, top to bottom, these figures are (1) the fraction of the population that is susceptible to the disease, (2) the fraction of the population that is infected, (3) the fraction of the population that has had the disease and recovered, (4) the fraction of the population that has died, and (5) the fraction of the population in quarantine.

Figure A.2: Scenario 2: Correctly Estimating the Pandemic

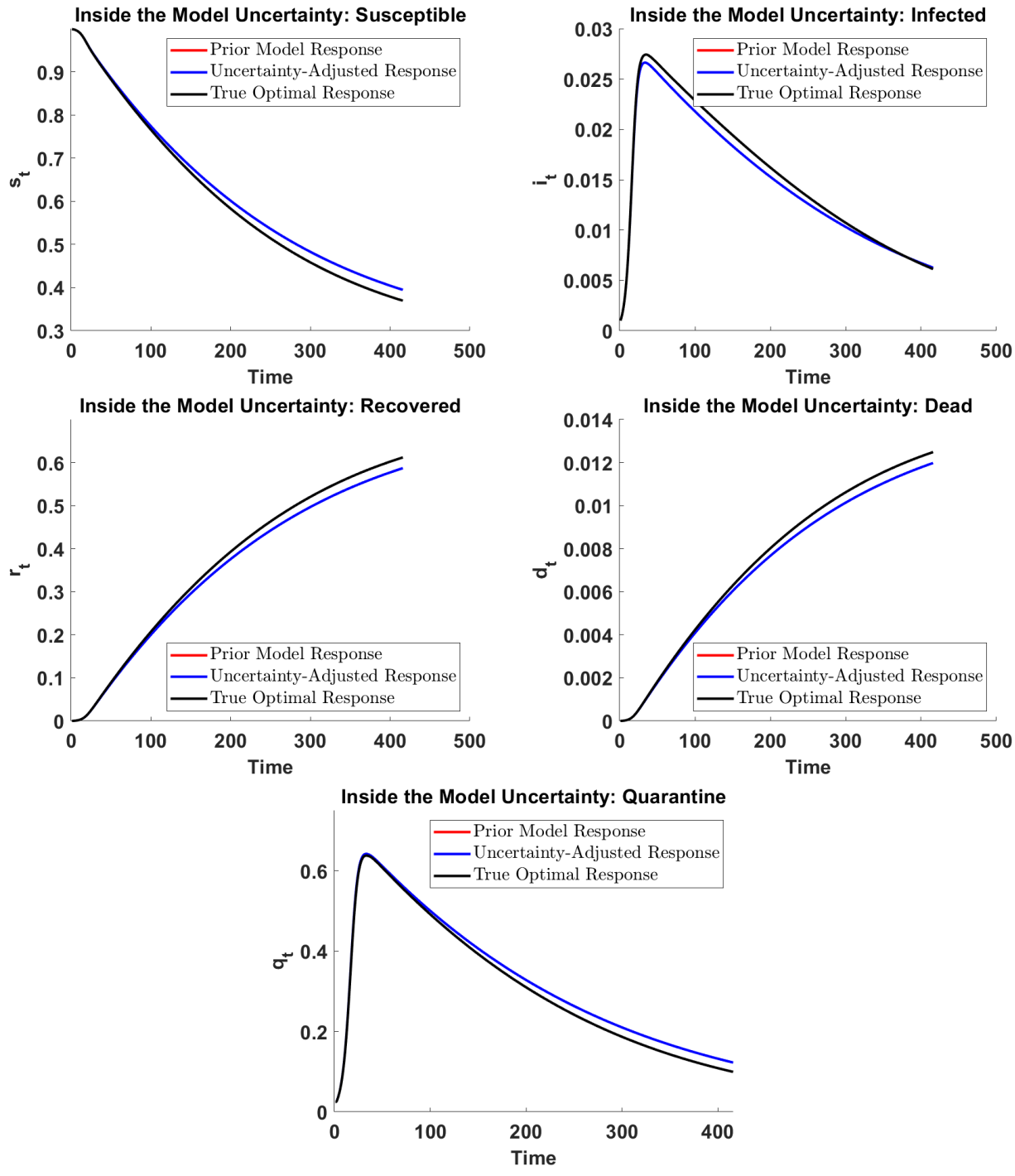

Notes: These figures show (i) the prior model response (red), the true optimal response (black), and the uncertainty-adjusted response (blue) in the case where the policy maker initially correctly estimates the severity of the pandemic. From left to right, top to bottom, these figures are (1) the fraction of the population that is susceptible to the disease, (2) the fraction of the population that is infected, (3) the fraction of the population that has had the disease and recovered, (4) the fraction of the population that has died, and (5) the fraction of the population in quarantine.

Figure A.3: Scenario 3: Overestimating the Pandemic

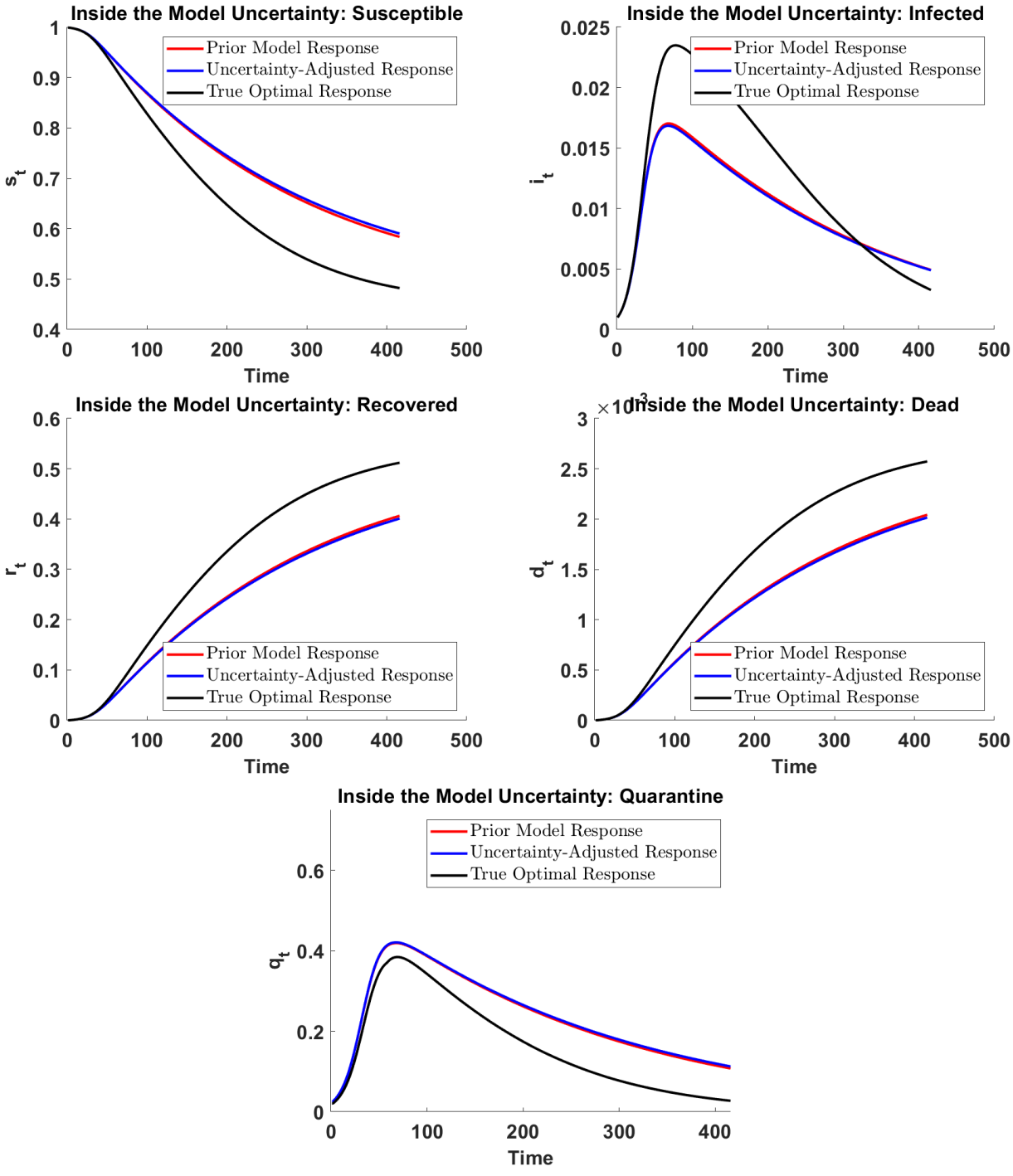

Notes: These figures show (i) the prior model response (red), the true optimal response (black), and the uncertainty-adjusted response (blue) in the case where the policy maker initially overestimates the severity of the pandemic. From left to right, top to bottom, these figures are (1) the fraction of the population that is susceptible to the disease, (2) the fraction of the population that is infected, (3) the fraction of the population that has had the disease and recovered, (4) the fraction of the population that has died, and (5) the fraction of the population in quarantine.